Adaptation of a snow cover scheme for complex topography areas: regional calibration over High Mountain Asia and application in global models

Mickaël Lalande, Martin Ménégoz, Gerhard Krinner, Catherine Ottlé

PhD Student 2019-2022
Institut des Géosciences de l'Environnement (IGE, Grenoble, France)

SnowHydro 2022 — 02/02/2022

High Mountain Asia (HMA): Introduction

- The Tibetan Plateau (TP): world's highest plateau (average elevation 4000m) → influence on regional and global climate (e.g., Kutzbach et al., 1993)
- Water supply of over 1.4 billion living downstream (e.g. Immerzeel et al., 2012)
- Climatic regimes:
  - winter westerly disturbances (WDs)
  - Indian / East Asian summer monsoon
- Warming over the HMA and TP (Liu et al., 2000; Wang et al., 2008) -> impacts on permafrost (Yang et al., 2010), glaciers (Yao et al., 2007), water resources (e.g. Immerzeel et al., 2010), etc.

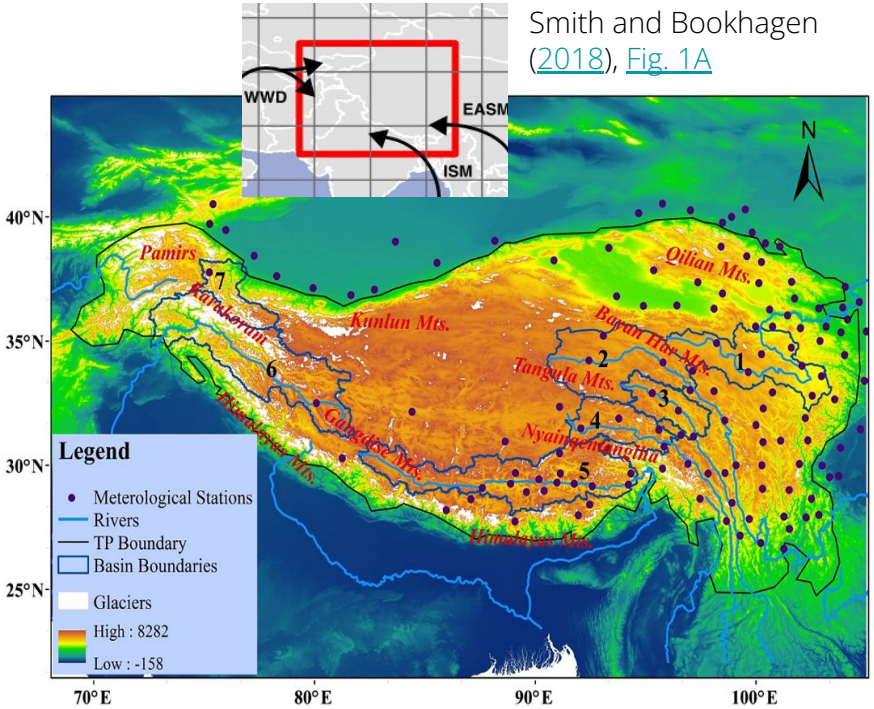

Smith and Bookhagen (2018), Fig. 1A

Li et al. (2018), Fig. 1

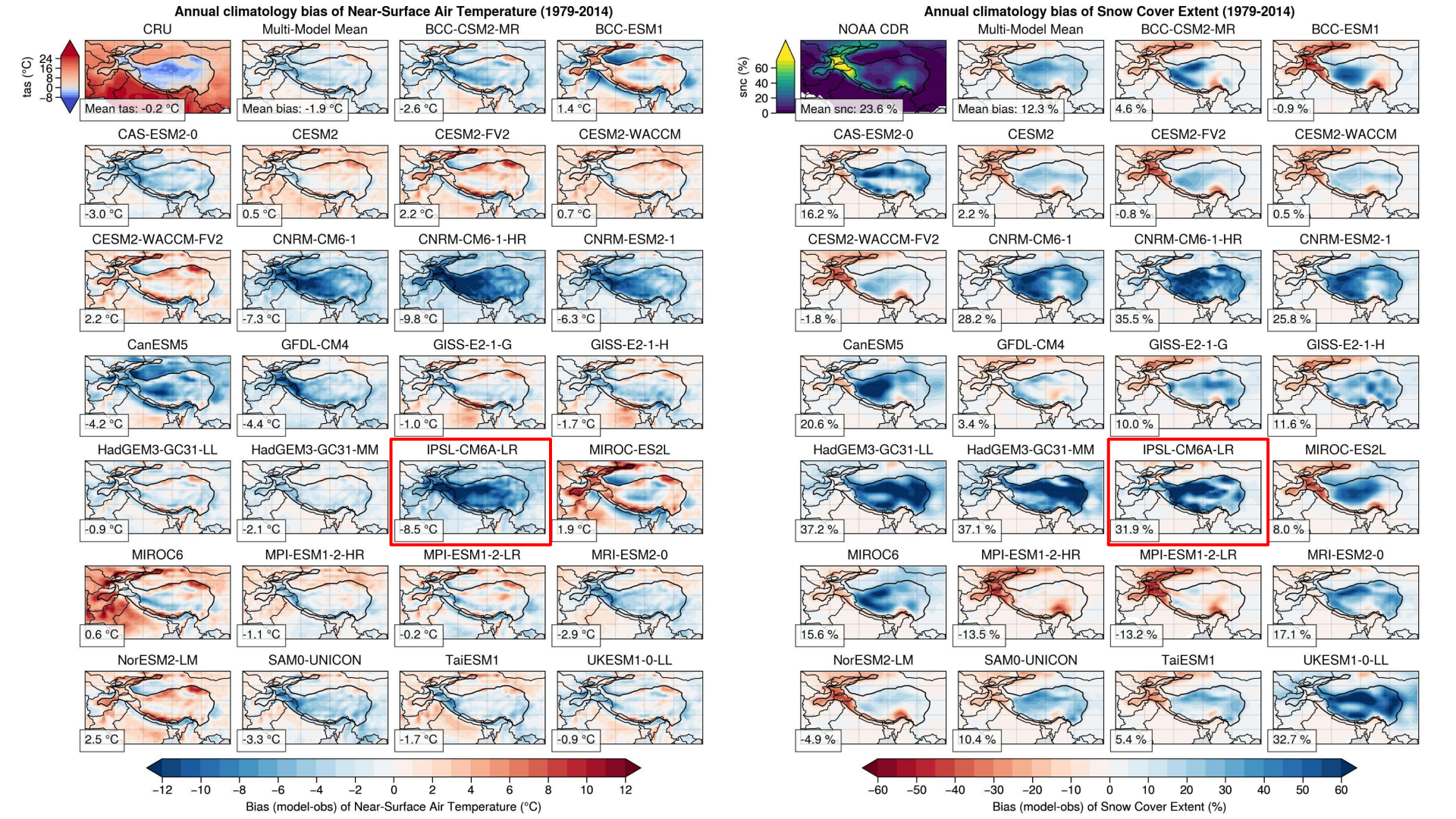
Annual climatology bias of Near-Surface Air Temperature (1979-2014)
CRU
Multi-Model Mean
BCC-CSM2-MR
BCC-ESM1
tas (°C)
24
16
8
0
−8
Mean tas: -0.2 °C
Mean bias: -1.9 °C
-2.6 °C
1.4 °C
CAS-ESM2-0
CESM2
CESM2-FV2
CESM2-WACCM
-3.0 °C
0.5 °C
2.2 °C
0.7 °C
CESM2-WACCM-FV2
CNRM-CM6-1
CNRM-CM6-1-HR
CNRM-ESM2-1
2.2 °C
-7.3 °C
-9.8 °C
-6.3 °C
CanESM5
GFDL-CM4
GISS-E2-1-G
GISS-E2-1-H
-4.2 °C
-4.4 °C
-1.0 °C
-1.7 °C
HadGEM3-GC31-LL
HadGEM3-GC31-MM
IPSL-CM6A-LR
MIROC-ES2L
-0.9 °C
-2.1 °C
-8.5 °C
1.9 °C
MIROC6
MPI-ESM1-2-HR
MPI-ESM1-2-LR
MRI-ESM2-0
0.6 °C
-1.1 °C
-0.2 °C
-2.9 °C
NorESM2-LM
SAM0-UNICON
TaiESM1
UKESM1-0-LL
2.5 °C
-3.3 °C
-1.7 °C
-0.9 °C
−12 −10 −8 −6 −4 −2 0 2 4 6 8 10 12
Bias (model-obs) of Near-Surface Air Temperature (°C)
Annual climatology bias of Snow Cover Extent (1979-2014)
NOAA CDR
Multi-Model Mean
BCC-CSM2-MR
BCC-ESM1
snc (%)
60
40
20
0
Mean snc: 23.6 %
Mean bias: 12.3 %
4.6 %
-0.9 %
CAS-ESM2-0
CESM2
CESM2-FV2
CESM2-WACCM
16.2 %
2.2 %
-0.8 %
0.5 %
CESM2-WACCM-FV2
CNRM-CM6-1
CNRM-CM6-1-HR
CNRM-ESM2-1
-1.8 %
28.2 %
35.5 %
25.8 %
CanESM5
GFDL-CM4
GISS-E2-1-G
GISS-E2-1-H
20.6 %
3.4 %
10.0 %
11.6 %
HadGEM3-GC31-LL
HadGEM3-GC31-MM
IPSL-CM6A-LR
MIROC-ES2L
37.2 %
37.1 %
31.9 %
8.0 %
MIROC6
MPI-ESM1-2-HR
MPI-ESM1-2-LR
MRI-ESM2-0
15.6 %
-13.5 %
-13.2 %
17.1 %
NorESM2-LM
SAM0-UNICON
TaiESM1
UKESM1-0-LL
-4.9 %
10.4 %
5.4 %
32.7 %
−60 −50 −40 −30 −20 −10 0 10 20 30 40 50 60
Bias (model-obs) of Snow Cover Extent (%)

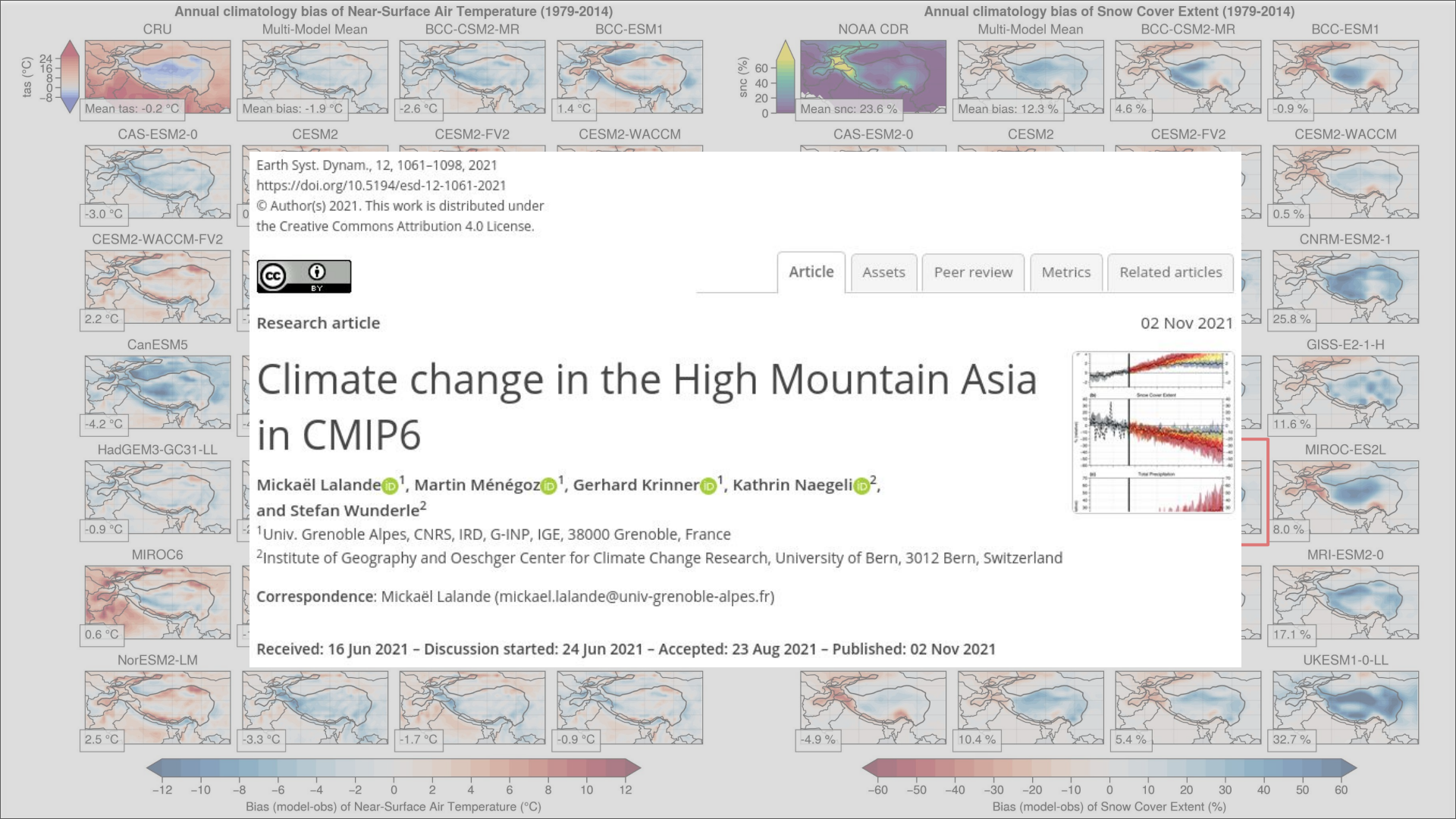

Earth Syst. Dynam., 12, 1061–1098, 2021
https://doi.org/10.5194/esd-12-1061-2021

Research article

02 Nov 2021

Climate change in the High Mountain Asia in CMIP6

Mickaël Lalande[1], **Martin Ménégoz**[1], **Gerhard Krinner**[1], **Kathrin Naegeli**[2], **and Stefan Wunderle**[2]

[1]Univ. Grenoble Alpes, CNRS, IRD, G-INP, IGE, 38000 Grenoble, France
[2]Institute of Geography and Oeschger Center for Climate Change Research, University of Bern, 3012 Bern, Switzerland

Correspondence: Mickaël Lalande (mickael.lalande@univ-grenoble-alpes.fr)

Received: 16 Jun 2021 – Discussion started: 24 Jun 2021 – Accepted: 23 Aug 2021 – Published: 02 Nov 2021

Snow cover parameterization in global models

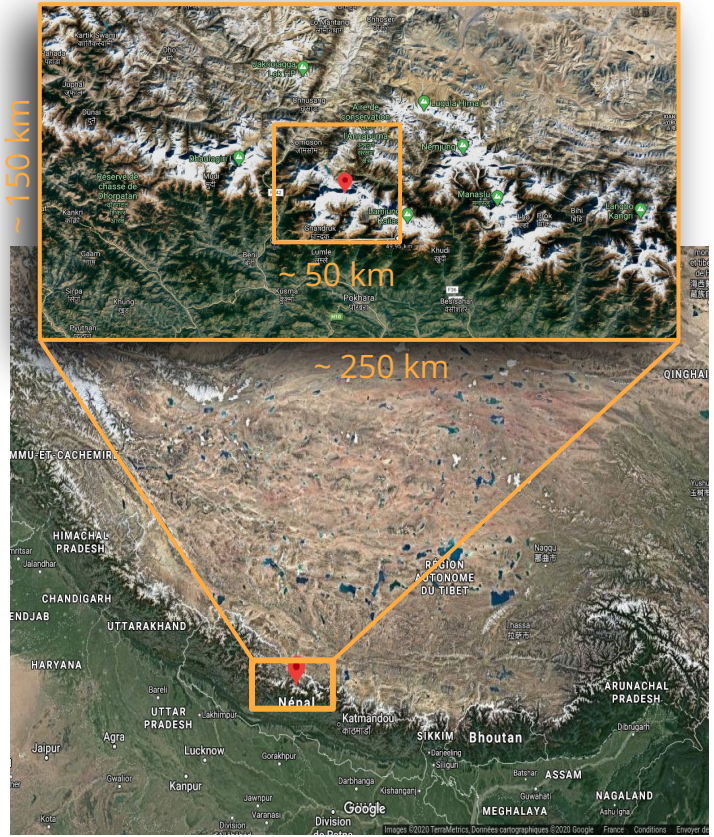

IPSL-CM6A

Snow cover parameterization in global models

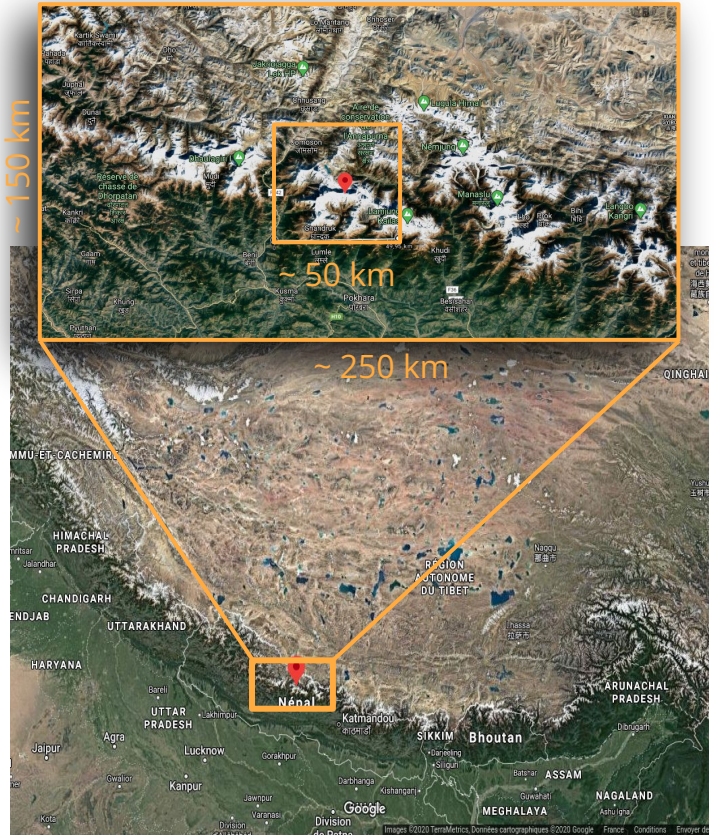

IPSL-CM6A

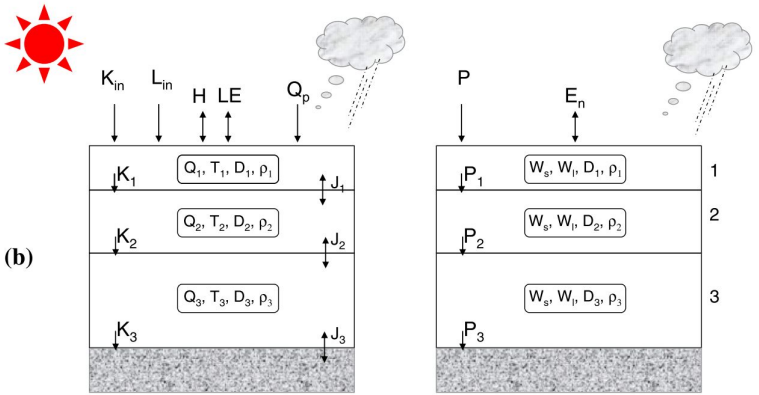

K_{in} (short wave radiation), **L_{in}** (longwave radiation), **H** (sensible heat flux), **LE**(latent heat flux), **J** (conduction heat flux), **Q** (snow layer heat content), **Q_p**(advective heat from rain and snow), **W** (snow layer SWE), **W_l** (snow layer liquid water content), **D** (snow layer depth), **ρ** (snow layer density) , **P** (precipitation), **E_n** (evaporation)

snow scheme in the ORCHIDEE land surface model (Wang et al., 2013)

Snow cover parameterization in global models

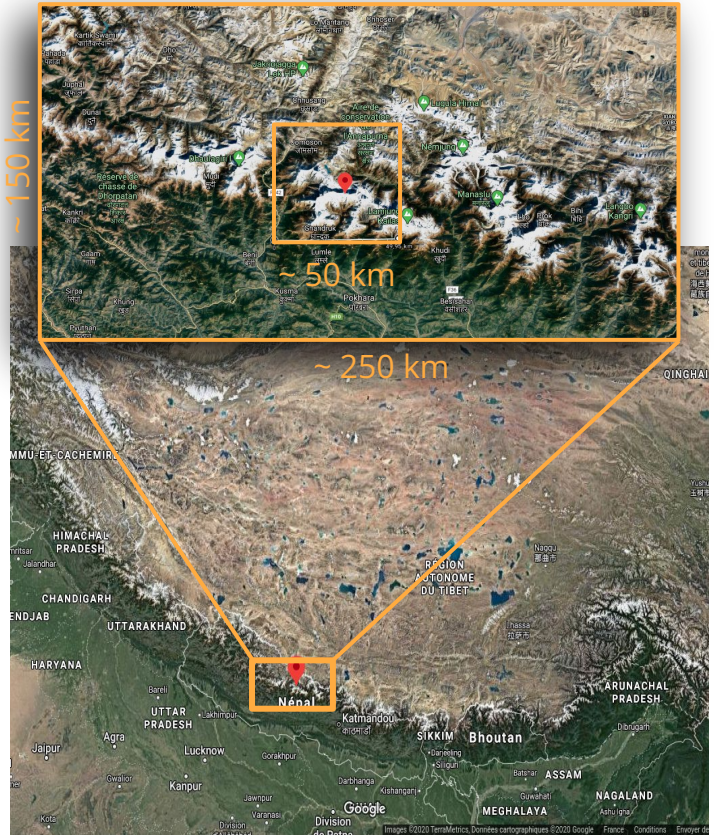

IPSL-CM6A

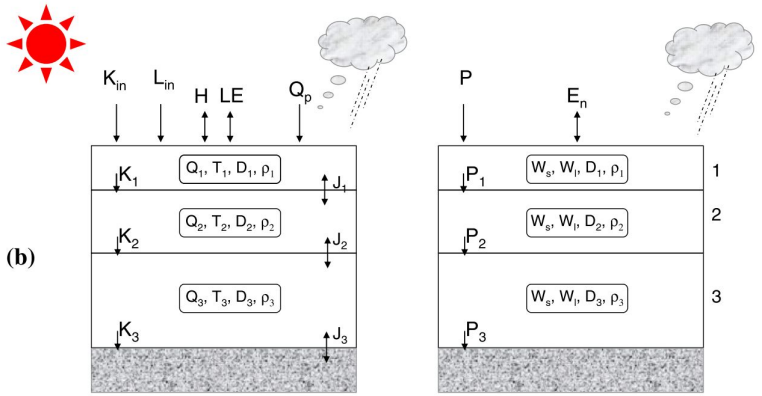

$\mathbf{K_{in}}$ (short wave radiation), $\mathbf{L_{in}}$ (longwave radiation), **H** (sensible heat flux), **LE**(latent heat flux), **J** (conduction heat flux), **Q** (snow layer heat content), $\mathbf{Q_p}$(advective heat from rain and snow), **W** (snow layer SWE), $\mathbf{W_l}$ (snow layer liquid water content), **D** (snow layer depth), **ρ** (snow layer density) , **P** (precipitation), $\mathbf{E_n}$ (evaporation)

snow scheme in the ORCHIDEE land surface model (Wang et al., 2013)

Snow Depth

Snow Water Equivalent

Snow Density

Snow cover parameterization in global models

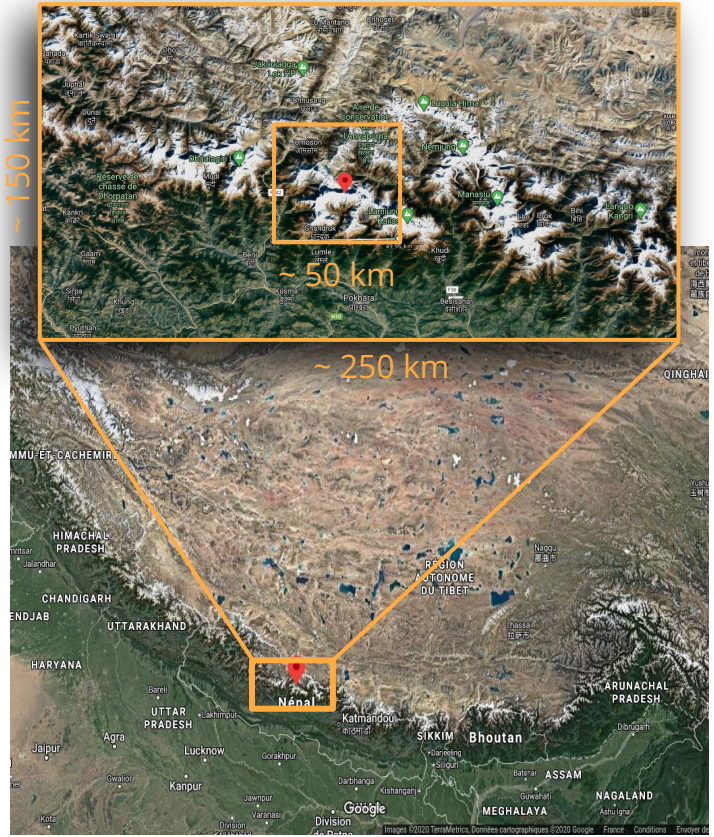

IPSL-CM6A

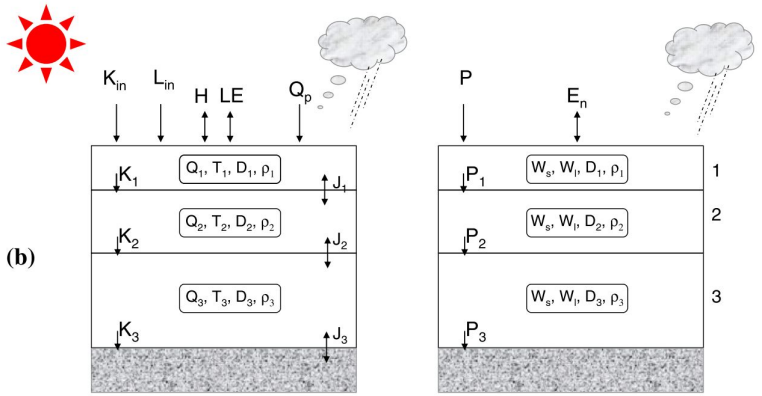

K_{in} (short wave radiation), **L_{in}** (longwave radiation), **H** (sensible heat flux), **LE**(latent heat flux), **J** (conduction heat flux), **Q** (snow layer heat content), **Q_p**(advective heat from rain and snow), **W** (snow layer SWE), **W_l** (snow layer liquid water content), **D** (snow layer depth), **ρ** (snow layer density) , **P** (precipitation), **E_n** (evaporation)

snow scheme in the ORCHIDEE land surface model (Wang et al., 2013)

Snow Depth

Snow Water Equivalent → Snow Cover Fraction

Snow Density

Snow cover real world vs global models

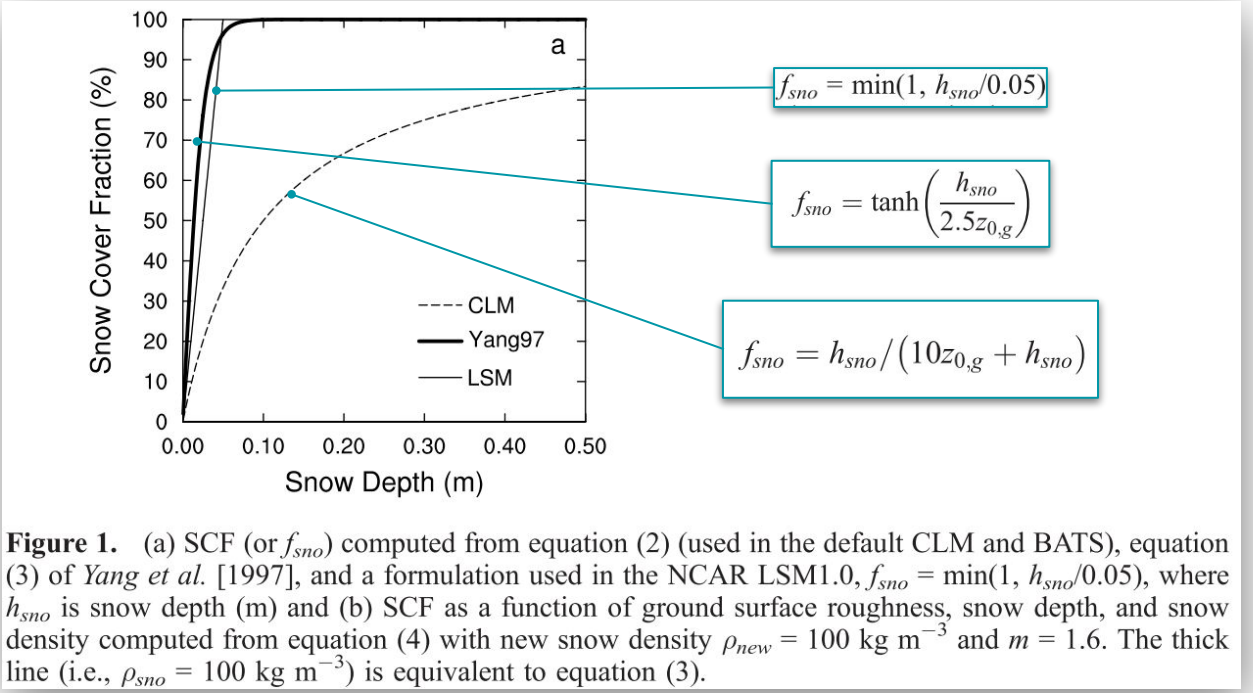

Figure 1. (a) SCF (or f_{sno}) computed from equation (2) (used in the default CLM and BATS), equation (3) of *Yang et al.* [1997], and a formulation used in the NCAR LSM1.0, $f_{sno} = \min(1, h_{sno}/0.05)$, where h_{sno} is snow depth (m) and (b) SCF as a function of ground surface roughness, snow depth, and snow density computed from equation (4) with new snow density $\rho_{new} = 100$ kg m^{-3} and $m = 1.6$. The thick line (i.e., $\rho_{sno} = 100$ kg m^{-3}) is equivalent to equation (3).

Niu and Yang (2007)

Snow Cover parameterization: Niu and Yang (2007)

$$f_{sno} = \tanh\left(\frac{h_{sno}}{2.5 z_{0g}(\rho_{sno}/\rho_{new})^{m}}\right)$$

Snow Density

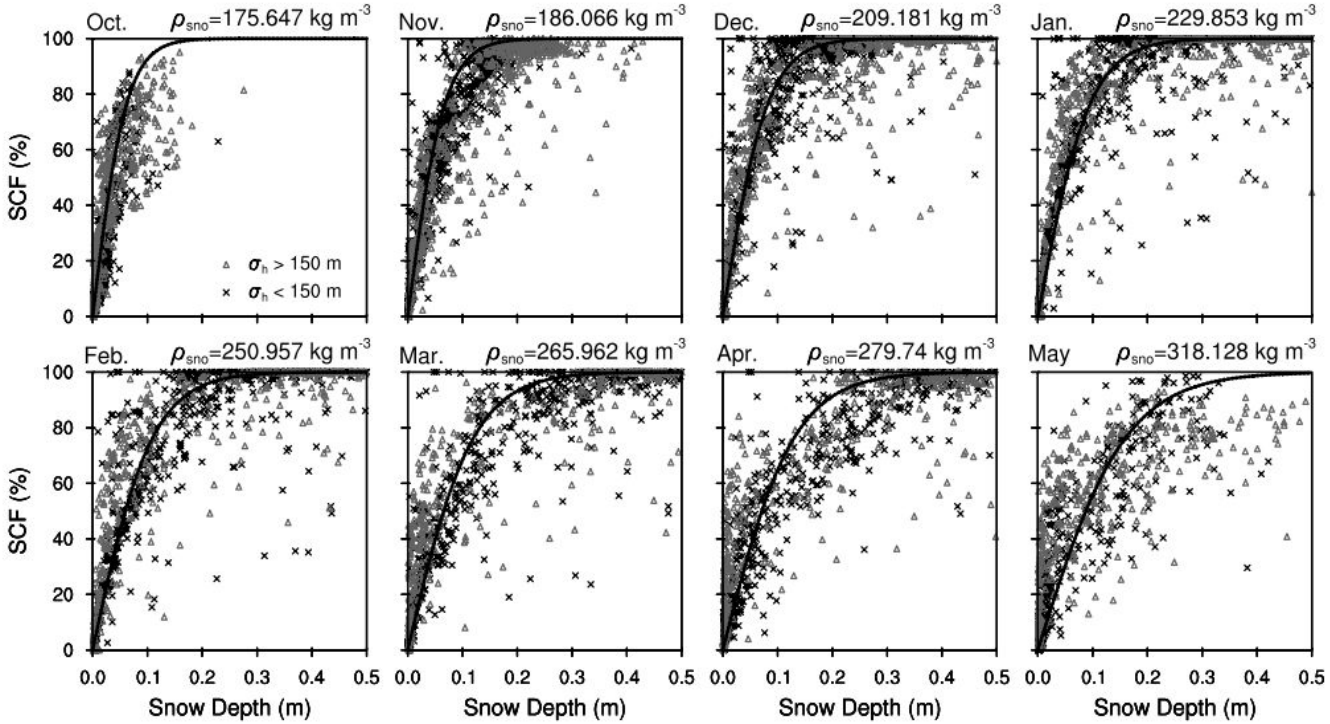

Figure 2. Relationship between AVHRR SCF (%) and CMC snow depth (m) in 1° × 1° grid cells of major NA river basins including the Mackenzie, Yukon, Churchill, Fraser, St. Lawrence, Columbia, Colorado, and Mississippi from October to May. The darker crosses stand for 1° × 1° grid cells where the standard deviation of topography $\sigma_h < 150$ m, and the lighter triangles stand for 1° × 1° grid cells where $\sigma_h > 150$ m. The fitted lines are computed from equation (4) ($m = 1.6$) with the mean snow densities shown above each frame.

Snow Cover parameterization: Niu and Yang (2007)

$$f_{sno} = \tanh\left(\frac{h_{sno}}{2.5z_{0g}(\rho_{sno}/\rho_{new})^{m}}\right)$$

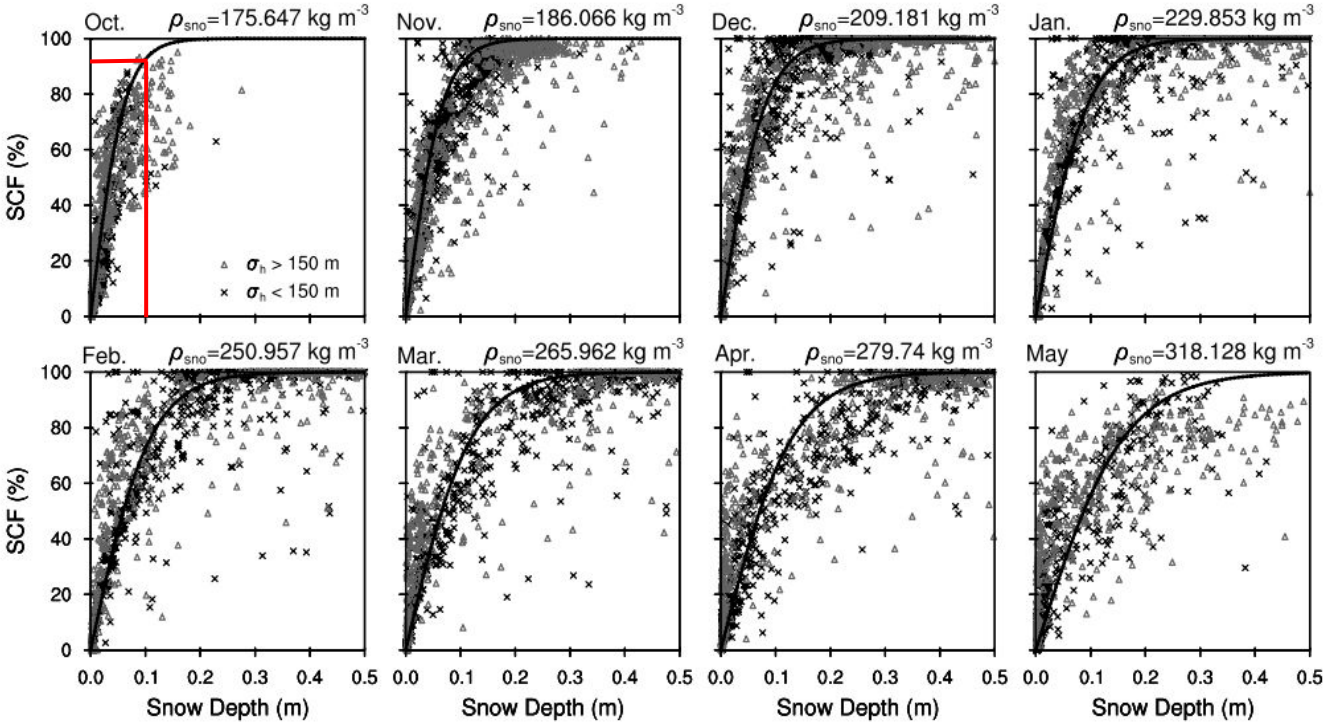

Figure 2. Relationship between AVHRR SCF (%) and CMC snow depth (m) in 1° × 1° grid cells of major NA river basins including the Mackenzie, Yukon, Churchill, Fraser, St. Lawrence, Columbia, Colorado, and Mississippi from October to May. The darker crosses stand for 1° × 1° grid cells where the standard deviation of topography $\sigma_h < 150$ m, and the lighter triangles stand for 1° × 1° grid cells where $\sigma_h > 150$ m. The fitted lines are computed from equation (4) ($m = 1.6$) with the mean snow densities shown above each frame.

Snow Cover parameterization: Niu and Yang (2007) - NY07

$$f_{sno} = \tanh\left(\frac{h_{sno}}{2.5 z_{0g}(\rho_{sno}/\rho_{new})^{m}}\right)$$

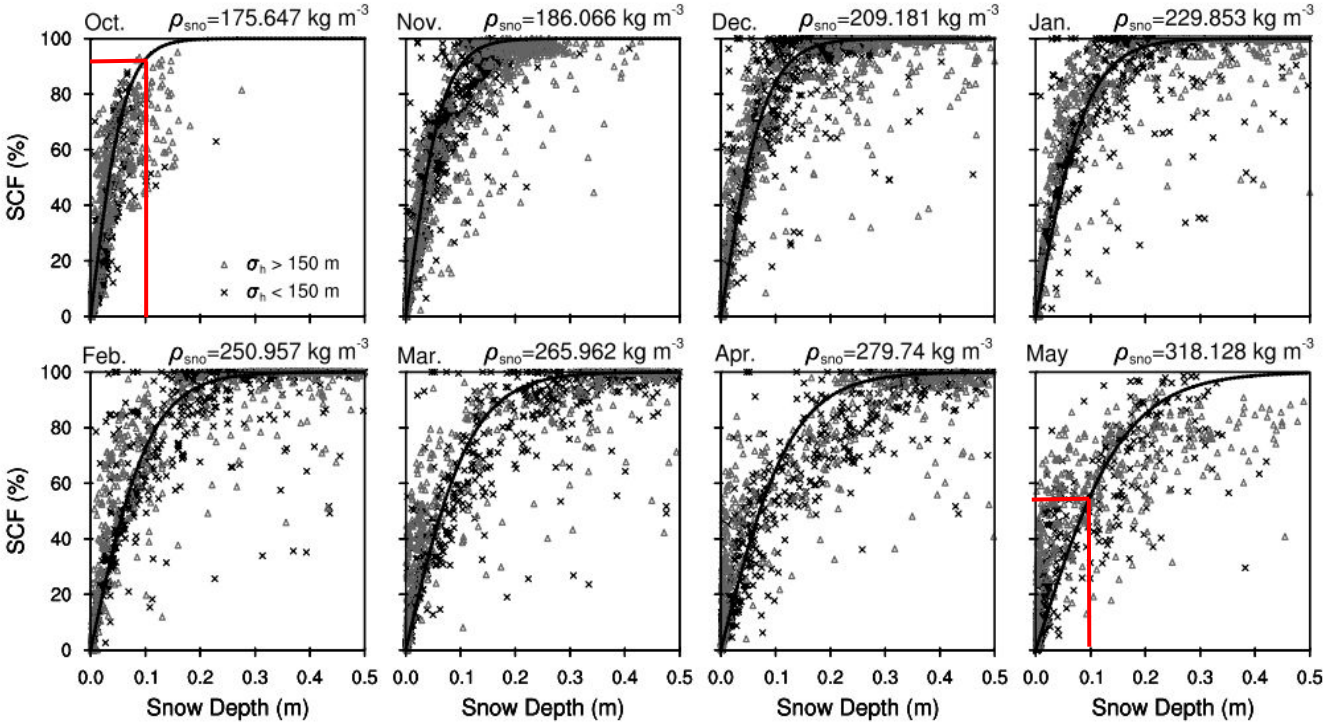

Figure 2. Relationship between AVHRR SCF (%) and CMC snow depth (m) in 1° × 1° grid cells of major NA river basins including the Mackenzie, Yukon, Churchill, Fraser, St. Lawrence, Columbia, Colorado, and Mississippi from October to May. The darker crosses stand for 1° × 1° grid cells where the standard deviation of topography $\sigma_h < 150$ m, and the lighter triangles stand for 1° × 1° grid cells where $\sigma_h > 150$ m. The fitted lines are computed from equation (4) ($m = 1.6$) with the mean snow densities shown above each frame.

Snow cover micro to macro

Snow cover micro to macro

Snow cover in mountainous area: Swenson & Lawrence (2012) - SL12

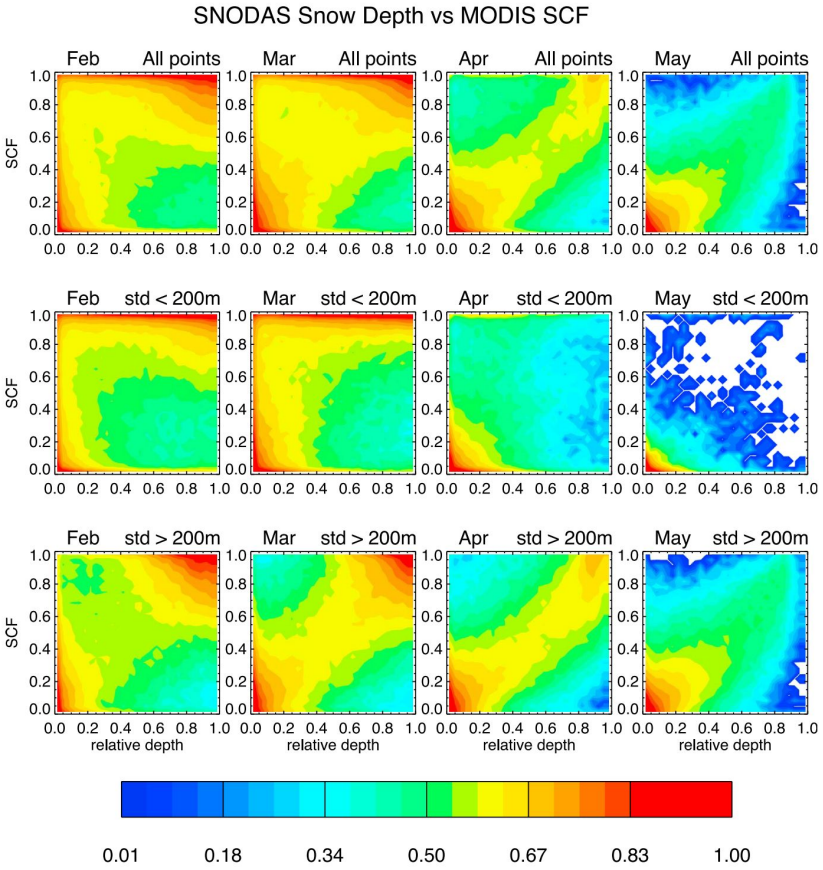

Swenson & Lawrence (2012)

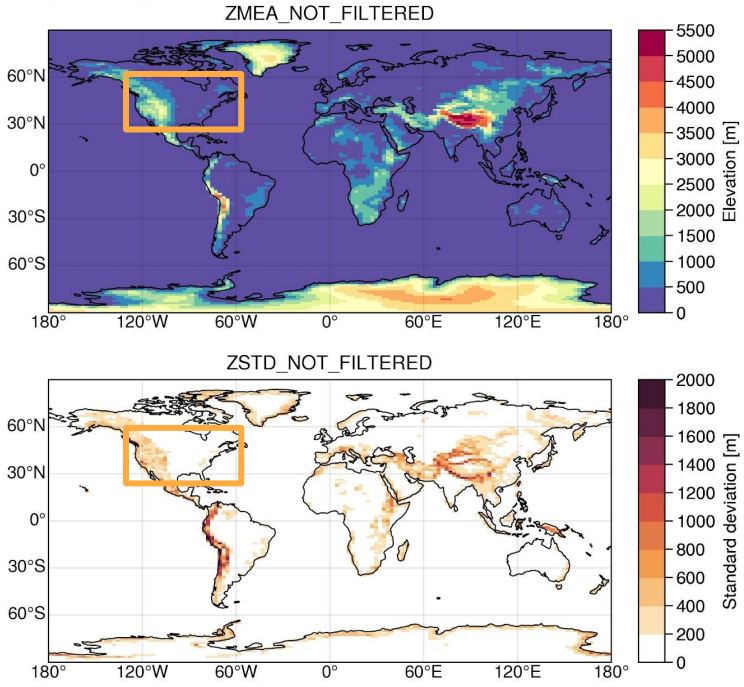

Snow cover in mountainous area: Swenson & Lawrence (2012)

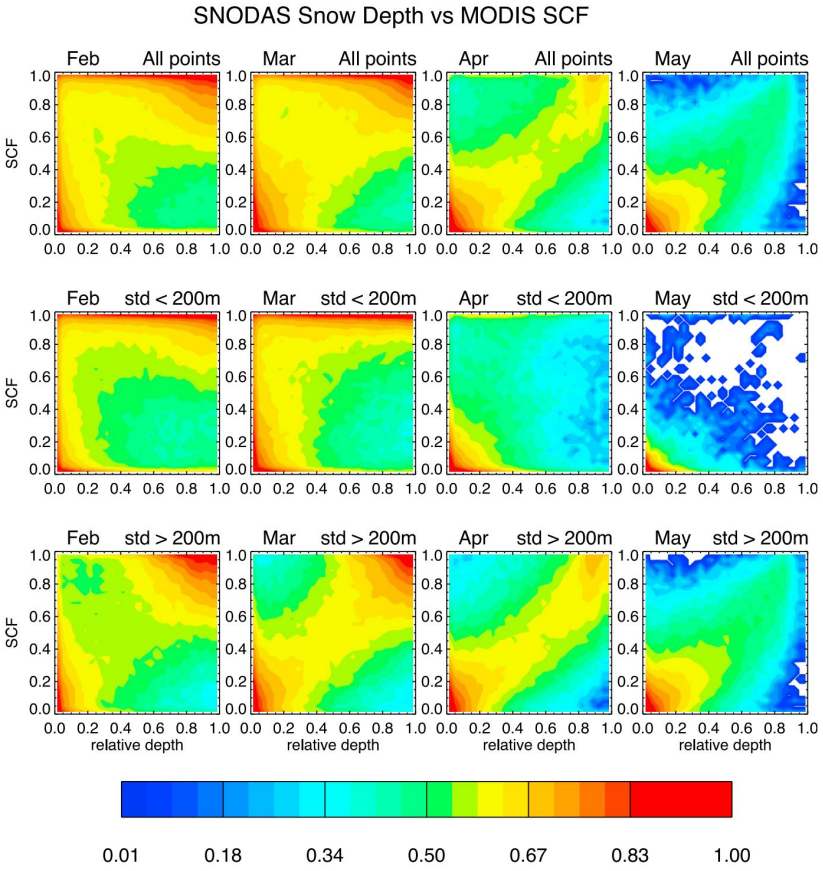

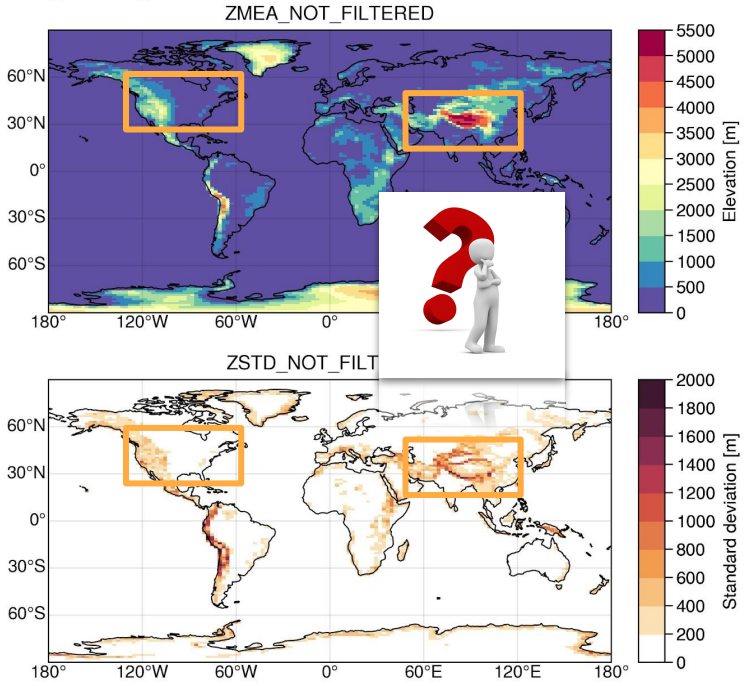

Swenson & Lawrence (2012)

High Mountain Asia UCLA Daily Snow Reanalysis (HMASR)

- **Problem**:
  - No global reliable product of SD/SWE over mountainous areas
  - To better test/calibrate SCF param -> need SD and SWE (or density)

High Mountain Asia UCLA Daily Snow Reanalysis (HMASR)

- **Problem**:
  - No global reliable product of SD/SWE over mountainous areas
  - To better test/calibrate SCF param -> need SD and SWE (or density)

- **New snow reanalysis over HMA**: HMASR
  - downscale meteorological forcing + topo/landcover -> prior SCF/SWE
  - assimilate Landsat/MODIS -> posterior SCF/SWE
  - provides daily SCF/SWE at 500 m
  - not validated over HMA / Sierra Nevada (Margulis et al., 2016) and Andes (Cortés and Margulis, 2017)

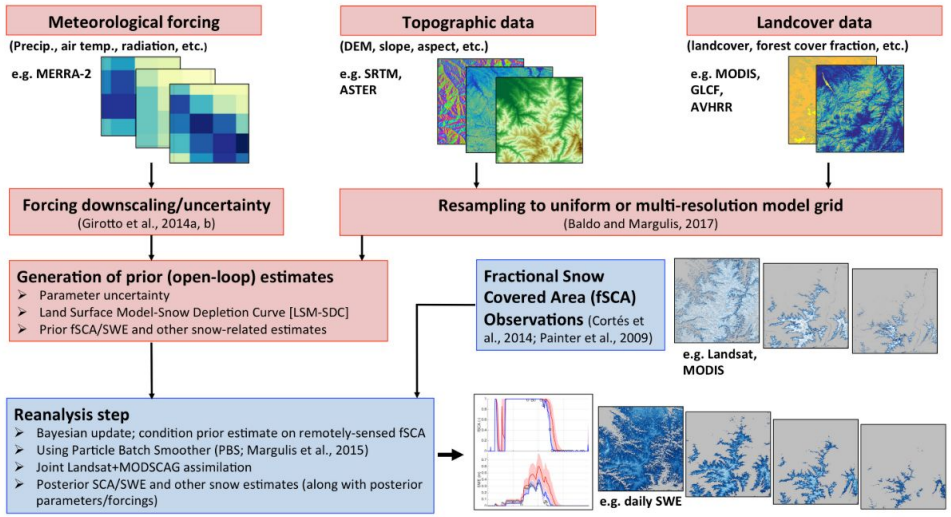

FIGURE 2 | Schematic representation of the Bayesian snow reanalysis framework that consists of an ensemble-based prior modeling system (red boxes) and a posterior update component for assimilating remotely sensed fractional snow covered area (SCA) data from Landsat and MODIS (blue boxes).

Margulis et al. (2019)

High Mountain Asia UCLA Daily Snow Reanalysis (HMASR)

- **Problem**:
  - No global reliable product of SD/SWE over mountainous areas
  - To better test/calibrate SCF param -> need SD and SWE (or density)

- **New snow reanalysis over HMA**: HMASR
  - validation with in-situ SD stations
    - time series correlation: 0.6
    - overestimation of SD
    - reproduce annual cycles
  - permanent snow not reliable -> use only seasonal snow

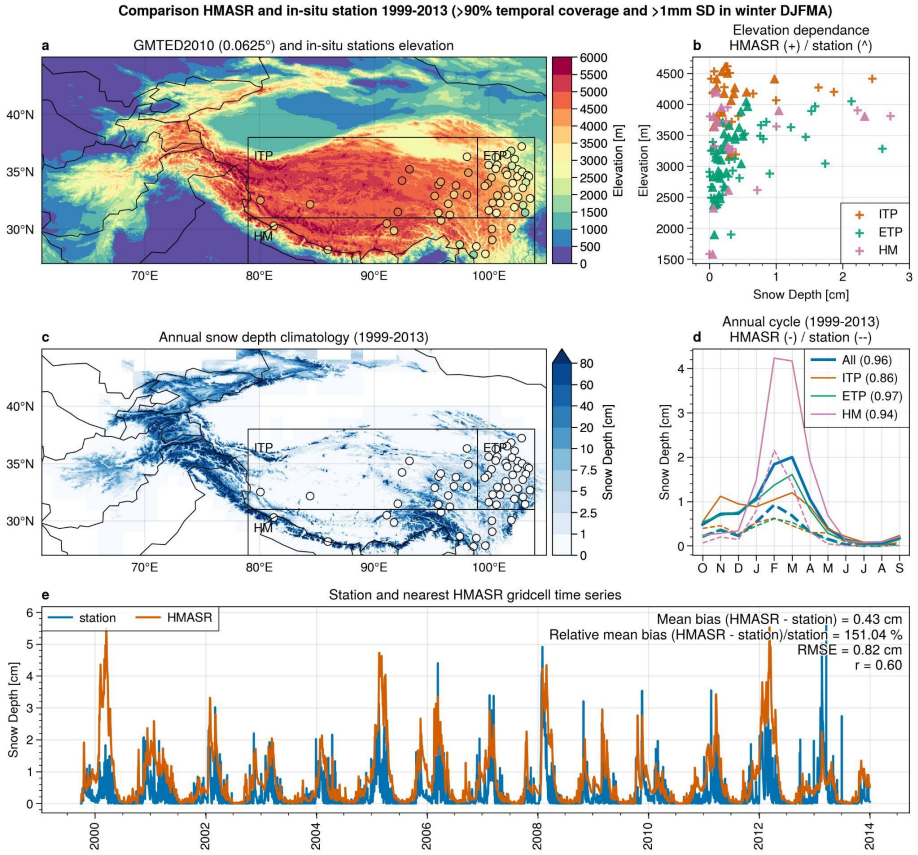

Snow cover in mountainous area: HMASR

$$f_{sno} = \tanh\left(\frac{h_{sno}}{2.5 z_{0g} (\rho_{sno}/\rho_{new})^m}\right)$$

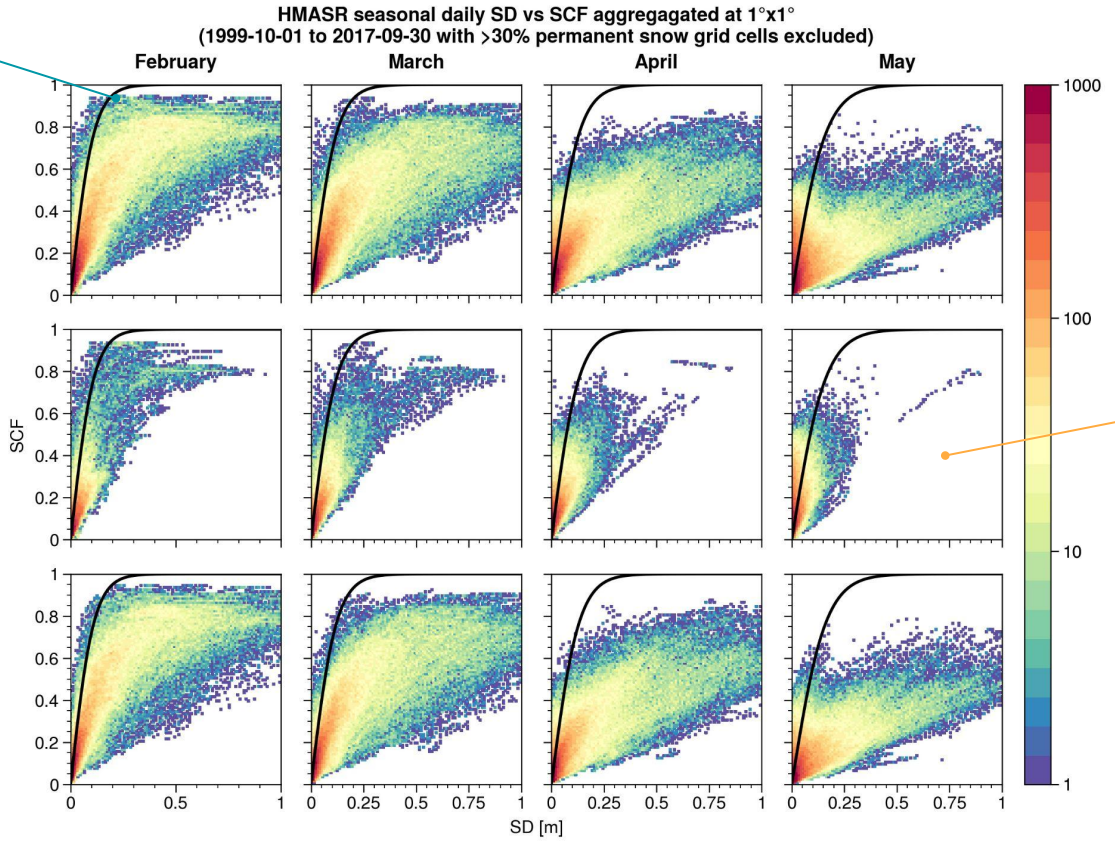

HMASR might be not representative of flat areas (TP mostly have STD >200m and dry)

Other snow cover parameterizations

Niu and Yang (2007) custom

$$F = \tanh\left(\frac{d}{2.5 z_{0g}(\rho_{snow}/\rho_{new})^{m}}\right)$$

STD topo

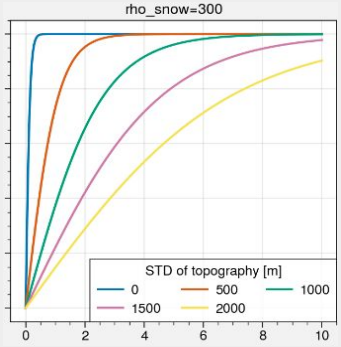

Swenson and Lawrence (2012)

Accumulation

$$F_{N+1} = 1 - (p_{N+1})(p_N) = 1 - (1 - s_{N+1})(1 - F_N)$$

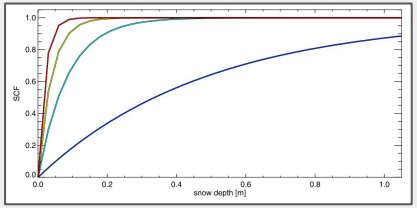

Depletion

$$F = 1 - \left[\frac{1}{\pi}\text{acos}\left(2\frac{W}{W_{\max}} - 1\right)\right]^{N_{melt}}$$

$$N_{melt} = \frac{200}{\sigma_{topo}}$$

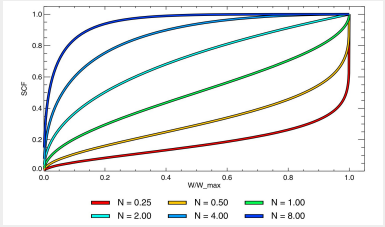

Roesch et al. (2001)

Mountainous areas

$$f_s = 0.95 \cdot tanh(100 \cdot S_n)\sqrt{\frac{1000 \cdot S_n}{1000 \cdot S_n + \epsilon + 0.15\sigma_z}}$$

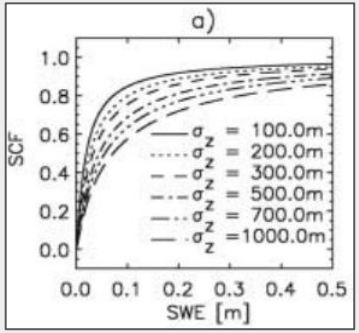

Depends only on SWE so no hysteresis

Preliminary test and calibration over small area

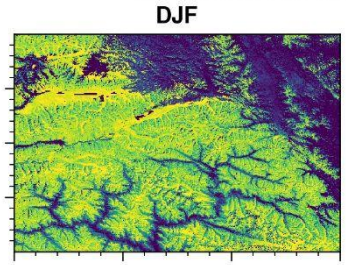

HMASR
SD / SWE / density / STD topo

SCF

Preliminary test and calibration over small area

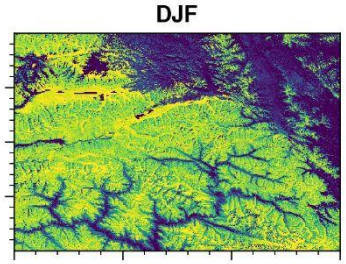

HMASR
SD / SWE / density / STD topo

SCF

$$f_{sno} = \tanh\left(\frac{h_{sno}}{2.5z_{0g}(\rho_{sno}/\rho_{new})^m}\right)$$

STD topo

$$f_s = 0.95 \cdot tanh(100 \cdot S_n)\sqrt{\frac{1000 \cdot S_n}{1000 \cdot S_n + \epsilon + 0.15\sigma_z}}$$

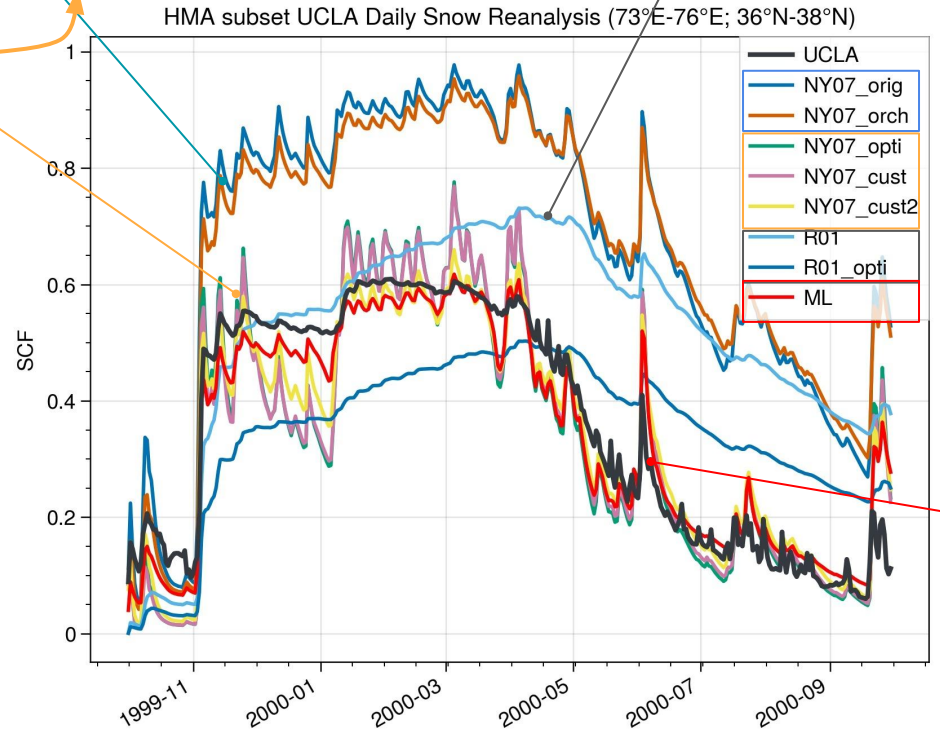

Calibration

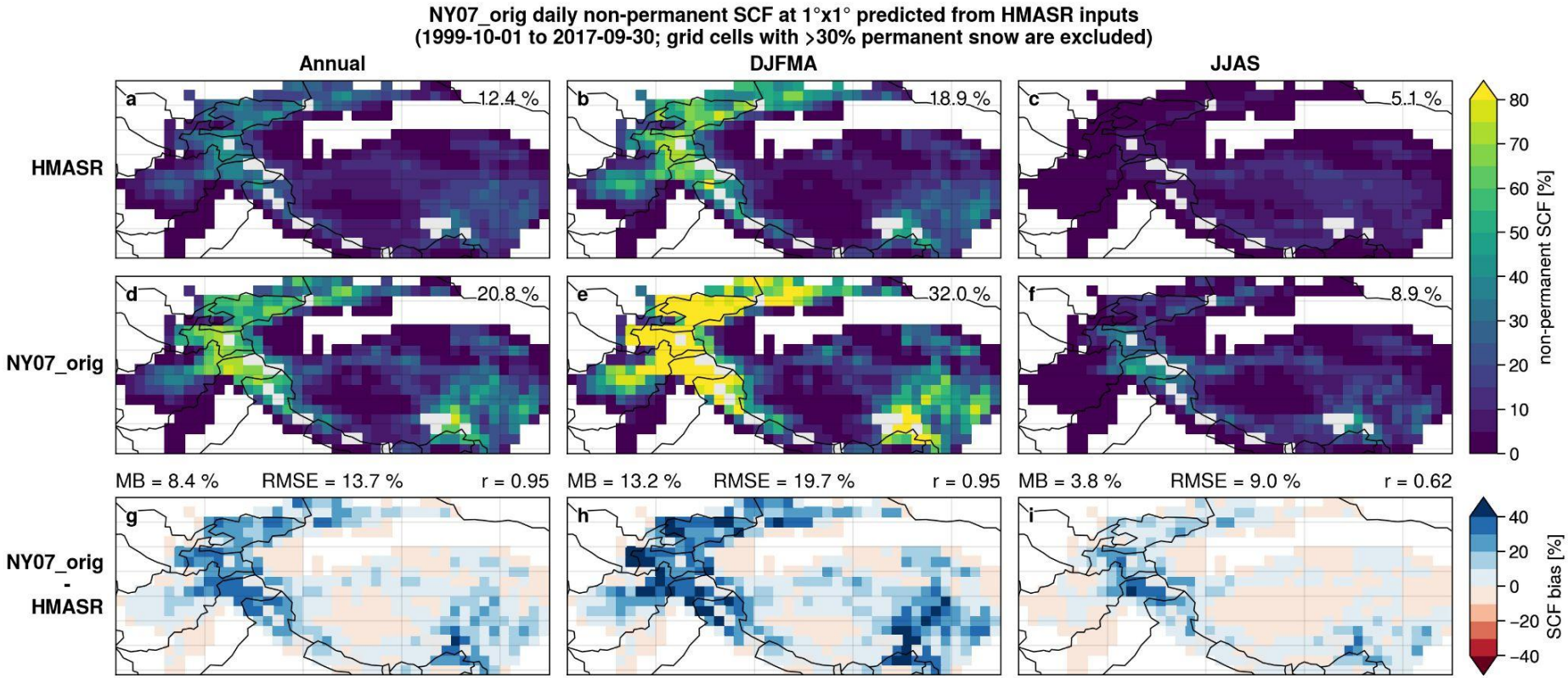

Calibration

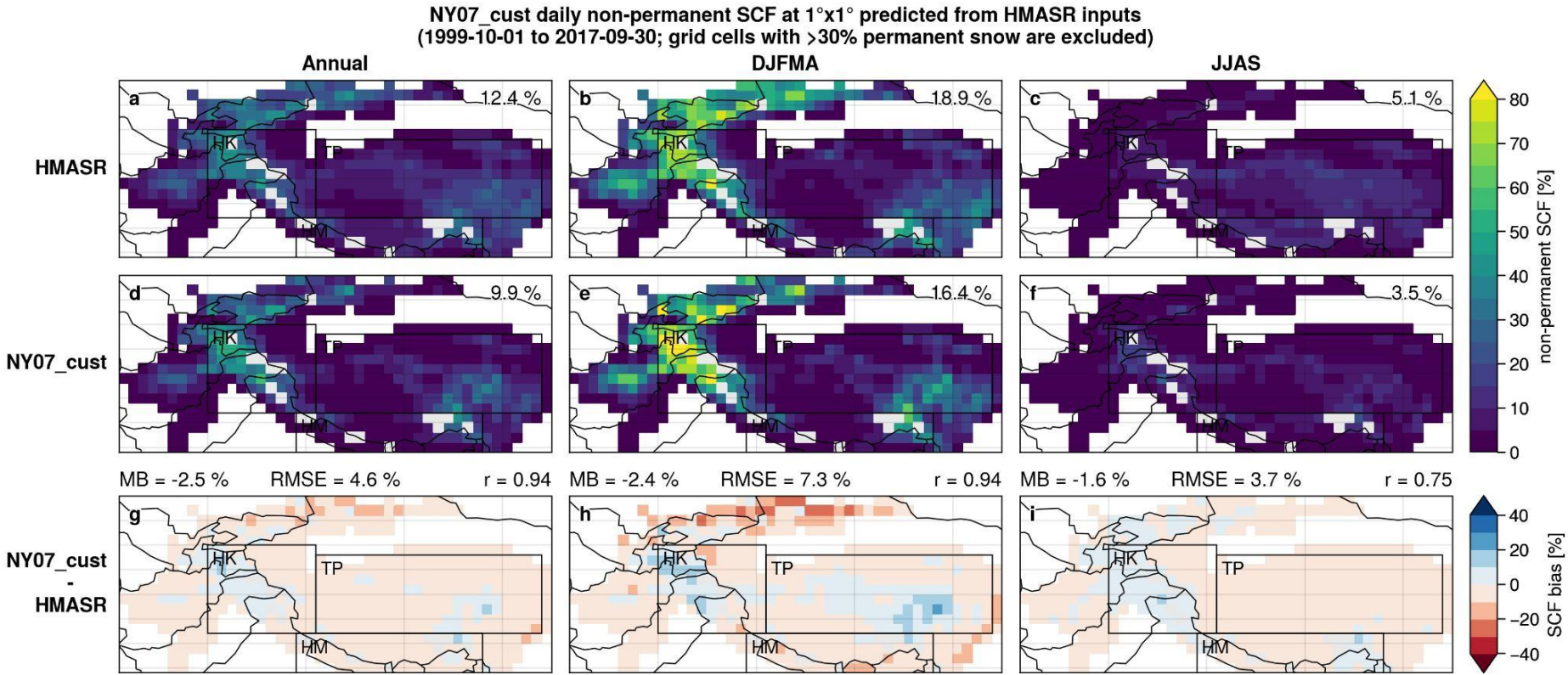

Niu and Yang (2007) custom

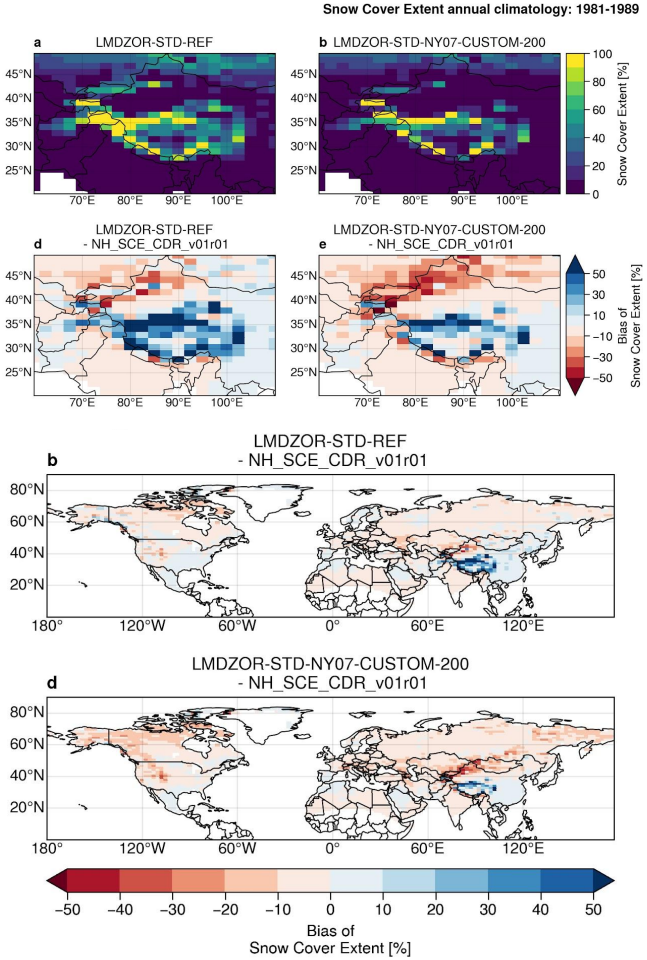

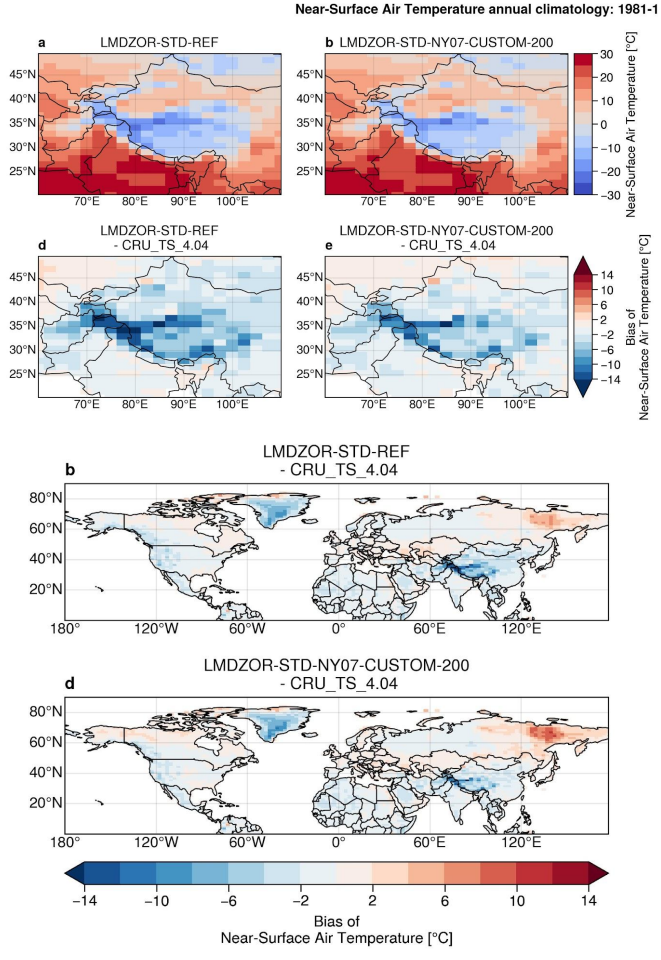

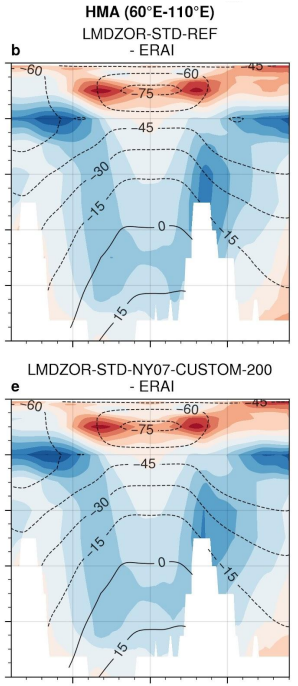

Perspectives / Discussion / Conclusion

- Finish to test SL12, R01, and ML over the whole HMA domain
- Test the sensitivity of the optimizations to the resolution (25, 50 and 100 km)
- Make simulation in ORCHIDEE with calibrated NY07_cust (+ nudged + zoom?)
- Not expected to fully solve the cold bias over HMA in ORCHIDEE:
    - precipitation (orographic drag; e.g, Wang et al., 2020) / aerosol deposition on snow (e.g., Usha et al., 2020) / boundary layer (e.g., Serafin et al., 2020) / tropospheric cold bias, etc.
- HMA not representative of flat areas (best would be to include other dataset from other areas)
- Permanent snow area could cause problem (-> accumulation/melt of snow over very small area -> glaciers)
    - elevation bands (e.g., Walland and Simmonds, 1996; Younas et al., 2017)
- Other parameterizations not tested, e.g.: Liston (2004), Helbig et al. (2021), etc.
- Deep learning very promising for these kind of parameterization

Bibliography

References

Cortés, G., & Margulis, S. (2017). Impacts of El Niño and La Niña on interannual snow accumulation in the Andes: Results from a high-resolution 31 year reanalysis. Geophysical Research Letters, 44(13), 6859–6867. https://doi.org/10.1002/2017GL073826

Helbig, N., van Herwijnen, A., Magnusson, J., & Jonas, T. (2015). Fractional snow-covered area parameterization over complex topography. Hydrology and Earth System Sciences, 19(3), 1339–1351. https://doi.org/10.5194/hess-19-1339-2015

Immerzeel, W. W., van Beek, L. P. H., & Bierkens, M. F. P. (2010). Climate Change Will Affect the Asian Water Towers. Science, 328(5984), 1382–1385. https://doi.org/10.1126/science.1183188

Immerzeel, W. W., & Bierkens, M. F. P. (2012). Asia's water balance. Nature Geoscience, 5(12), 841–842. https://doi.org/10.1038/ngeo1643

Kutzbach, J. E., Prell, W. L., & Ruddiman, W. F. (1993). Sensitivity of Eurasian Climate to Surface Uplift of the Tibetan Plateau. The Journal of Geology, 101(2), 177–190. https://doi.org/10.1086/648215

Lalande, M., Ménégoz, M., Krinner, G., Naegeli, K., & Wunderle, S. (2021). Climate change in the High Mountain Asia in CMIP6. Earth System Dynamics, 12(4), 1061–1098. https://doi.org/10.5194/esd-12-1061-2021

Li, C., Su, F., Yang, D., Tong, K., Meng, F., & Kan, B. (2018). Spatiotemporal variation of snow cover over the Tibetan Plateau based on MODIS snow product, 2001-2014. International Journal of Climatology, 38(2), 708–728. https://doi.org/10.1002/joc.5204

Liston, G. E. (2004). Representing Subgrid Snow Cover Heterogeneities in Regional and Global Models. Journal of Climate, 17(6), 1381–1397. https://doi.org/10.1175/1520-0442(2004)017<1381:RSSCHI>2.0.CO;2

Liu, X., & Chen, B. (2000). Climatic warming in the Tibetan Plateau during recent decades. International Journal of Climatology, 20(14), 1729–1742. https://doi.org/10.1002/1097-0088(20001130)20:14<1729::AID-JOC556>3.0.CO;2-Y

References

Liu, Y., Fang, Y., & Margulis, S. A. (2021). Spatiotemporal distribution of seasonal snow water equivalent in High Mountain Asia from an 18-year Landsat–MODIS era snow reanalysis dataset. The Cryosphere, 15(11), 5261–5280. https://doi.org/10.5194/tc-15-5261-2021

Margulis, S. A., Cortés, G., Girotto, M., & Durand, M. (2016). A Landsat-Era Sierra Nevada Snow Reanalysis (1985–2015). Journal of Hydrometeorology, 17(4), 1203–1221. https://doi.org/10.1175/JHM-D-15-0177.1

Margulis, S. A., Liu, Y., & Baldo, E. (2019). A Joint Landsat- and MODIS-Based Reanalysis Approach for Midlatitude Montane Seasonal Snow Characterization. Frontiers in Earth Science, 7(October), 1–23. https://doi.org/10.3389/feart.2019.00272

Niu, G.-Y., & Yang, Z.-L. (2007). An observation-based formulation of snow cover fraction and its evaluation over large North American river basins. Journal of Geophysical Research, 112(D21), D21101. https://doi.org/10.1029/2007JD008674

Roesch, A., Wild, M., Gilgen, H., & Ohmura, A. (2001). A new snow cover fraction parametrization for the ECHAM4 GCM. Climate Dynamics, 17(12), 933–946. https://doi.org/10.1007/s003820100153

Serafin, S., Rotach, M. W., Arpagaus, M., Colfescu, I., Cuxart, J., De Wekker, S. F. J., … Zardi, D. (2020). Multi-scale transport and exchange processes in the atmosphere over mountains. In Multi-scale transport and exchange processes in the atmosphere over mountains. https://doi.org/10.15203/99106-003-1

Smith, T., & Bookhagen, B. (2018). Changes in seasonal snow water equivalent distribution in High Mountain Asia (1987 to 2009). Science Advances, 4(1), e1701550. https://doi.org/10.1126/sciadv.1701550

Swenson, S. C., & Lawrence, D. M. (2012). A new fractional snow-covered area parameterization for the Community Land Model and its effect on the surface energy balance. Journal of Geophysical Research: Atmospheres, 117(D21), n/a-n/a. https://doi.org/10.1029/2012JD018178

References

Usha, K. H., Nair, V. S., & Babu, S. S. (2020). Modeling of aerosol induced snow albedo feedbacks over the Himalayas and its implications on regional climate. Climate Dynamics, (0123456789). https://doi.org/10.1007/s00382-020-05222-5

WALLAND, D. J., & SIMMONDS, I. (1996). SUB-GRID-SCALE TOPOGRAPHY AND THE SIMULATION OF NORTHERN HEMISPHERE SNOW COVER. International Journal of Climatology, 16(9), 961–982. http://doi.wiley.com/10.1002/%28SICI%291097-0088%28199609%2916%3A9%3C961%3A%3AAID-JOC72%3E3.0.CO%3B2-R

Wang, B., Bao, Q., Hoskins, B., Wu, G., & Liu, Y. (2008). Tibetan Plateau warming and precipitation changes in East Asia. Geophysical Research Letters, 35(14), L14702. https://doi.org/10.1029/2008GL034330

Wang, T., Ottlé, C., Boone, A., Ciais, P., Brun, E., Morin, S., … Peng, S. (2013). Evaluation of an improved intermediate complexity snow scheme in the ORCHIDEE land surface model. Journal of Geophysical Research: Atmospheres, 118(12), 6064–6079. https://doi.org/10.1002/jgrd.50395

Wang, Y., Yang, K., Zhou, X., Chen, D., Lu, H., Ouyang, L., … Wang, B. (2020). Synergy of orographic drag parameterization and high resolution greatly reduces biases of WRF-simulated precipitation in central Himalaya. Climate Dynamics, 54(3–4), 1729–1740. https://doi.org/10.1007/s00382-019-05080-w

Yang, M., Nelson, F. E., Shiklomanov, N. I., Guo, D., & Wan, G. (2010). Permafrost degradation and its environmental effects on the Tibetan Plateau: A review of recent research. Earth-Science Reviews, 103(1–2), 31–44. https://doi.org/10.1016/j.earscirev.2010.07.002

Yao, T., Pu, J., Lu, A., Wang, Y., & Yu, W. (2007). Recent glacial retreat and its impact on hydrological processes on the Tibetan Plateau, China, and surrounding regions. Arctic, Antarctic, and Alpine Research, 39(4), 642–650. https://doi.org/https://doi.org/10.1657/1523-0430(07-510)[YAO]2.0.CO;2

References

Younas, W., Hay, R. W., MacDonald, M. K., Islam, S. U., & Déry, S. J. (2017). A strategy to represent impacts of subgrid-scale topography on snow evolution in the Canadian Land Surface Scheme. Annals of Glaciology, 58(75pt1), 1–10. https://doi.org/10.1017/aog.2017.29

Complementary Slides

High Mountain Asia UCLA Daily Snow Reanalysis

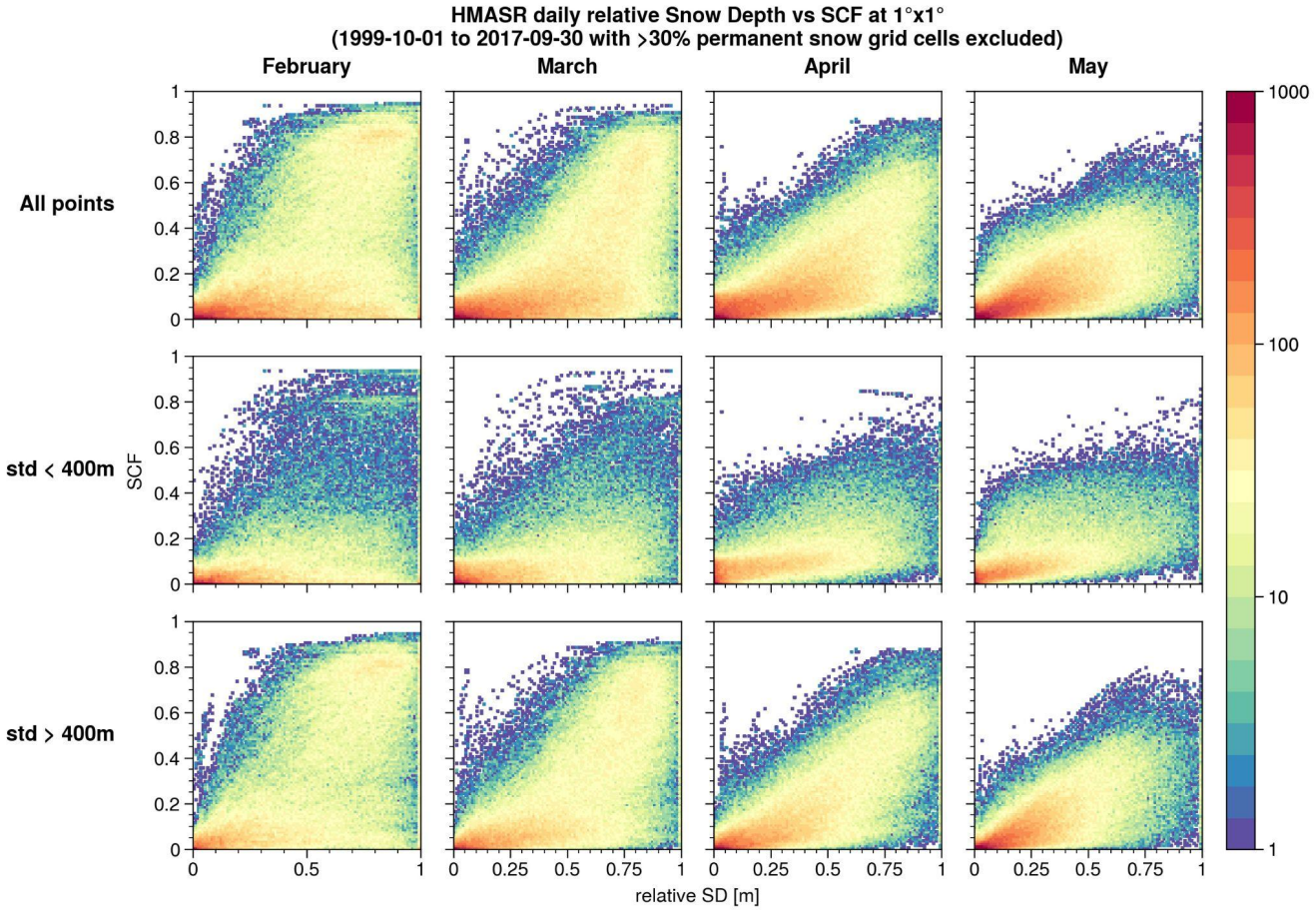

High Mountain Asia UCLA Daily Snow Reanalysis

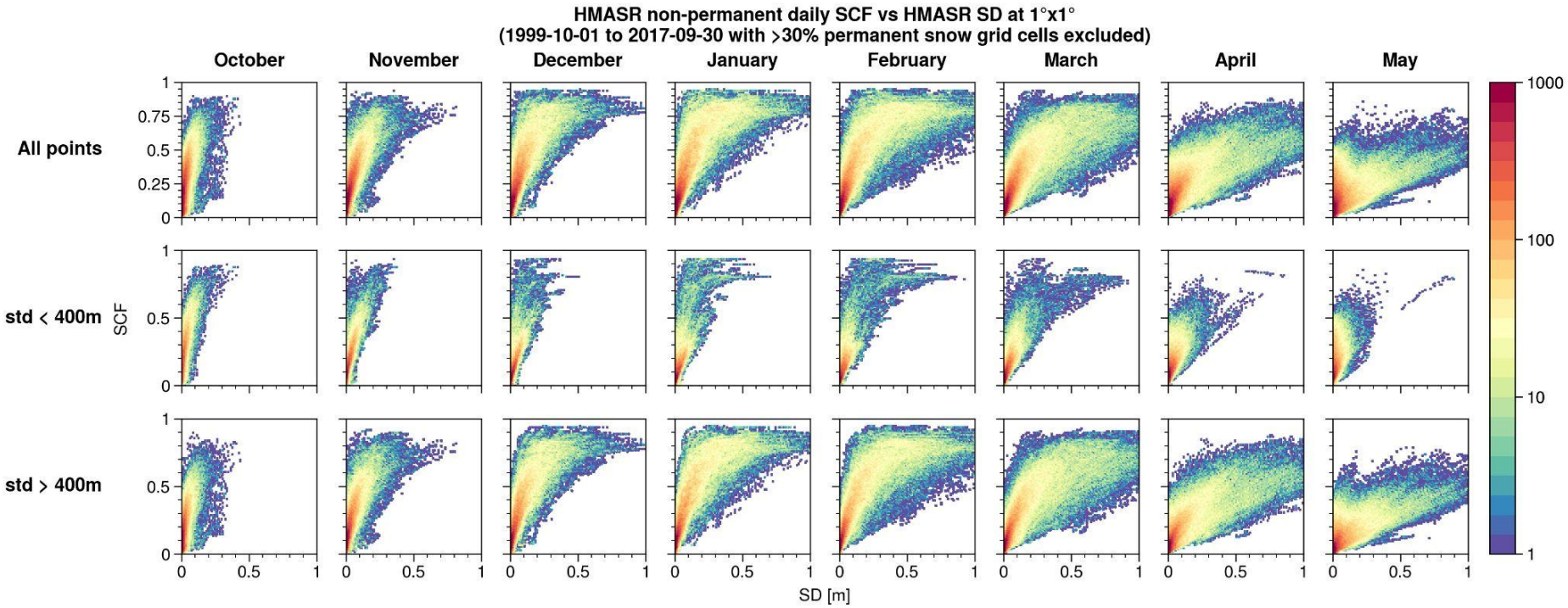

High Mountain Asia UCLA Daily Snow Reanalysis

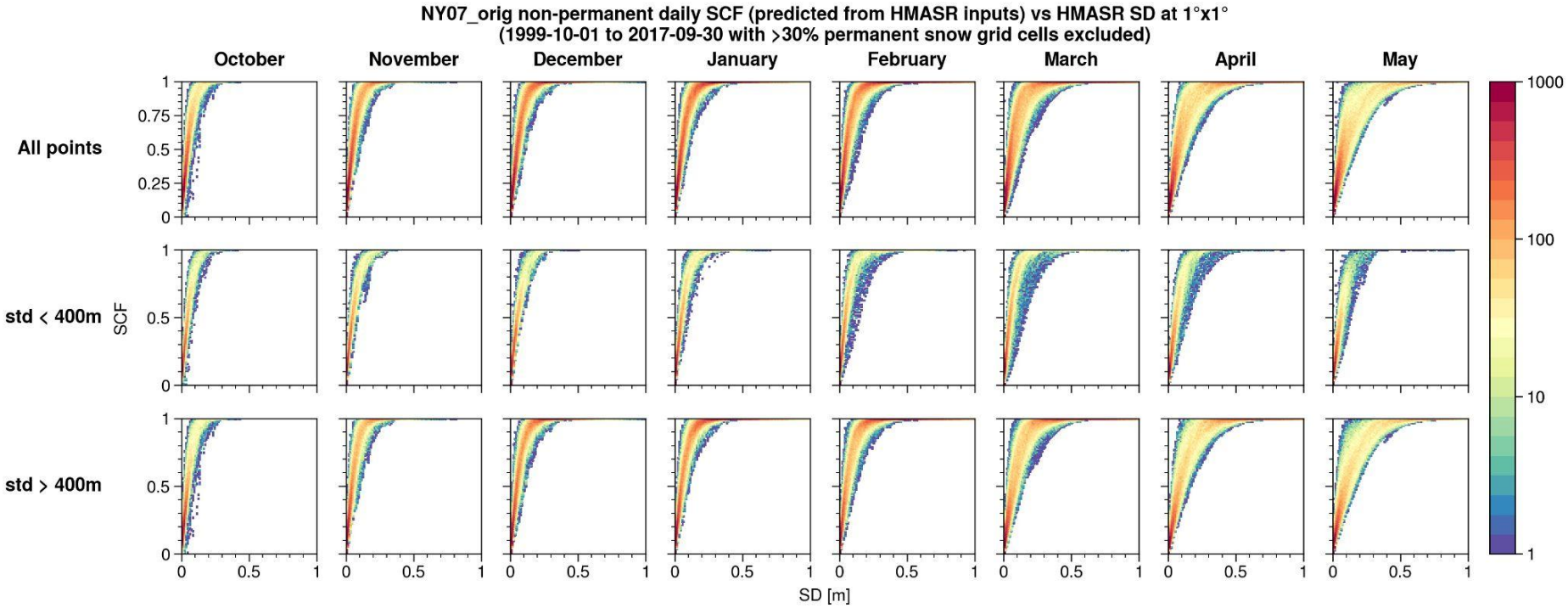

High Mountain Asia UCLA Daily Snow Reanalysis

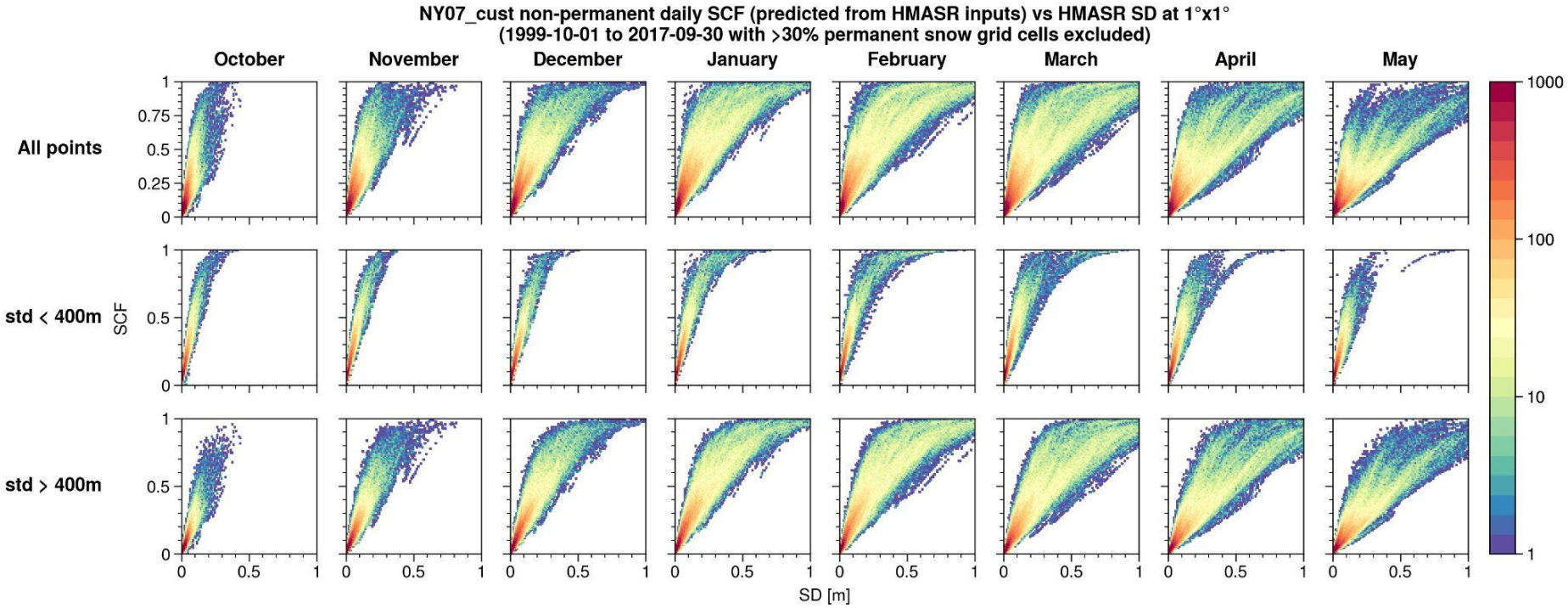

High Mountain Asia UCLA Daily Snow Reanalysis

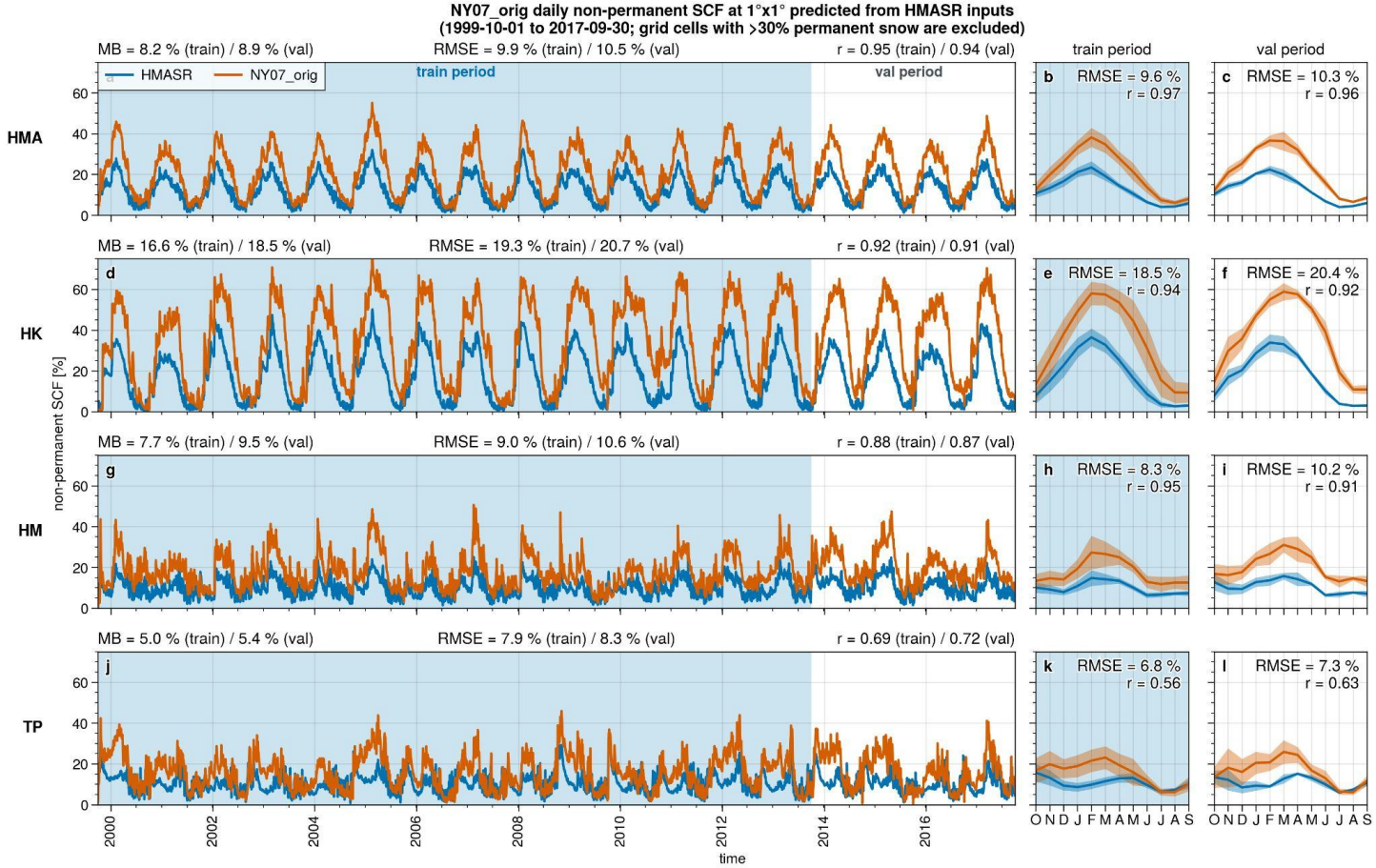

High Mountain Asia UCLA Daily Snow Reanalysis

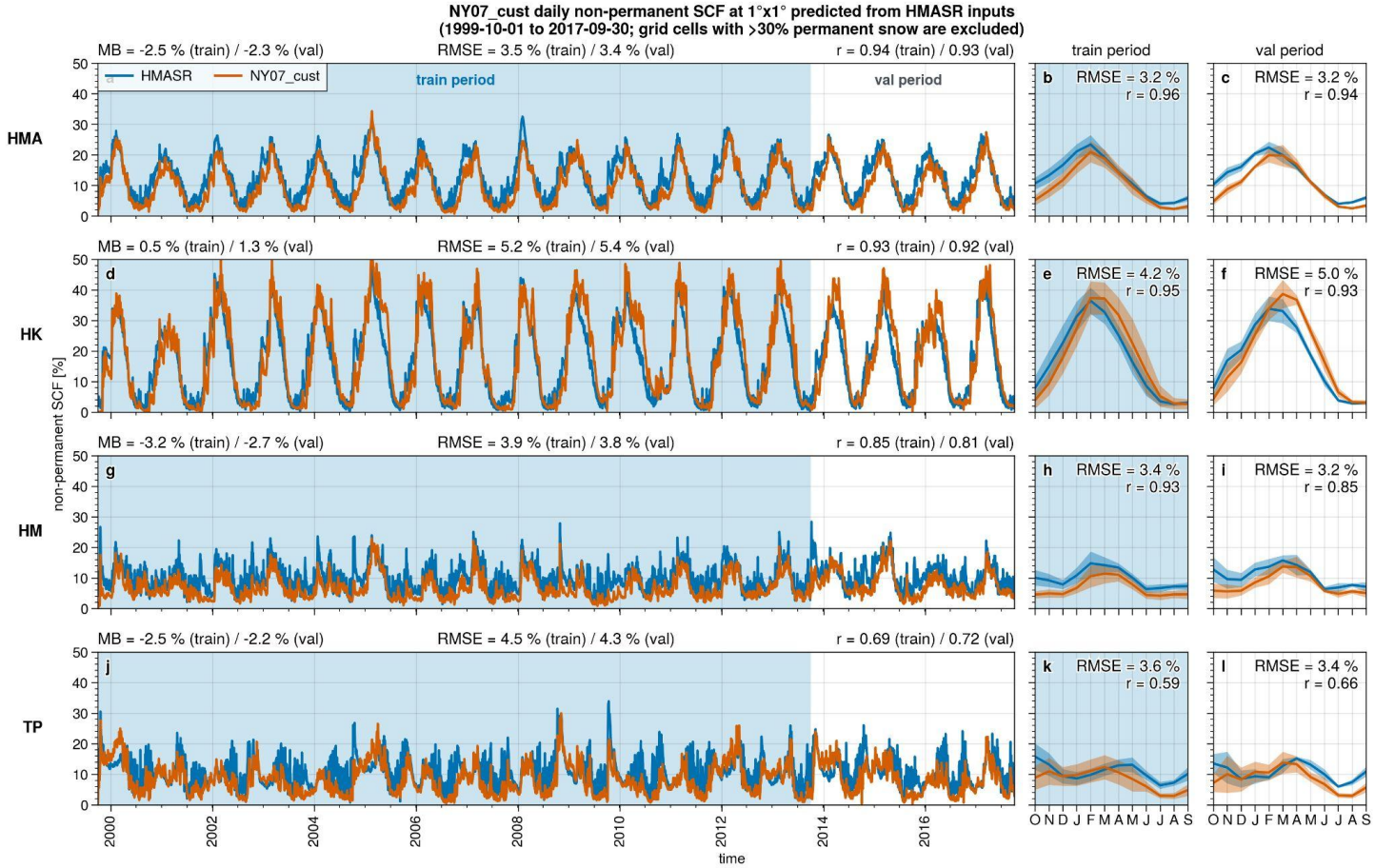

High Mountain Asia UCLA Daily Snow Reanalysis

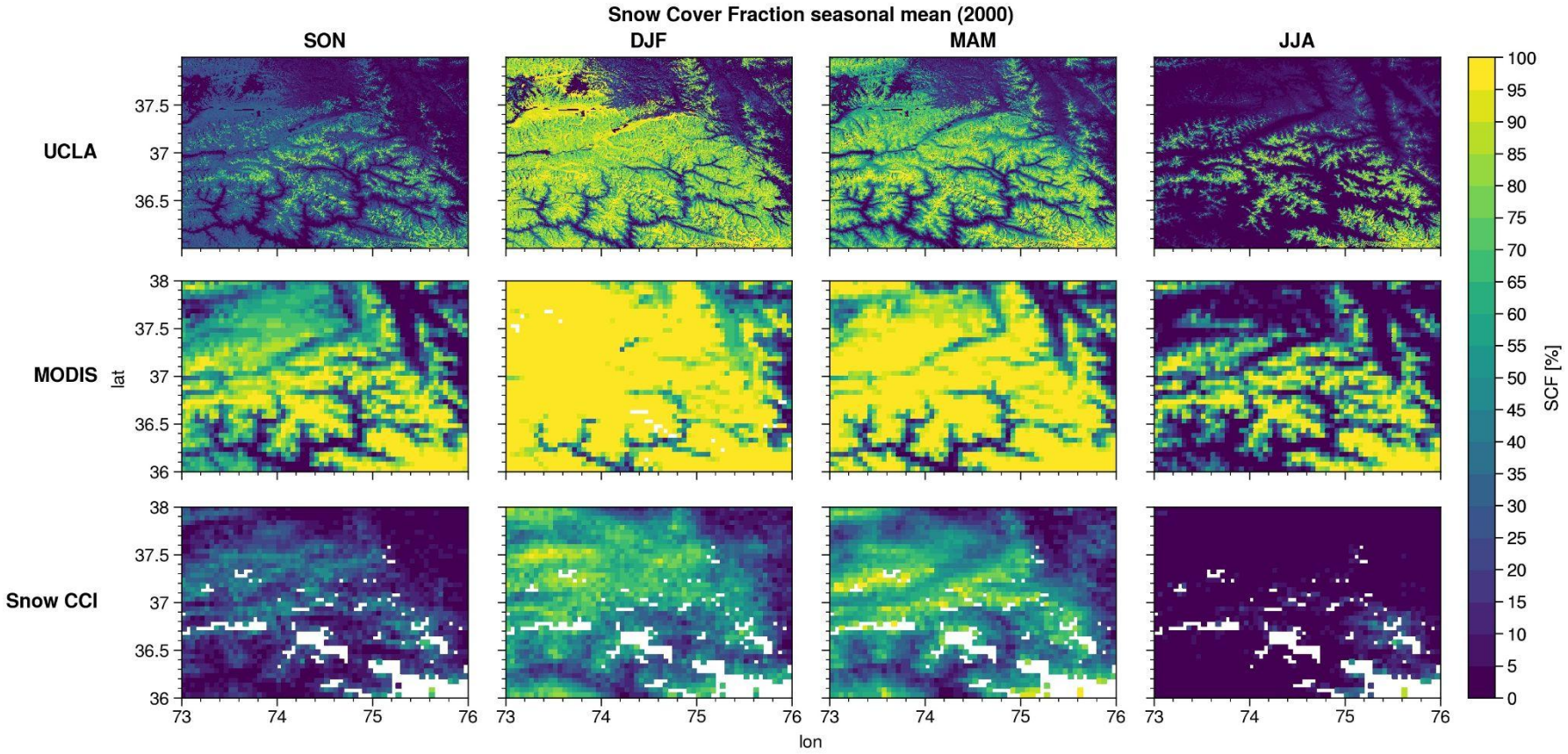

Deep learning NN

HMASR
SD / SWE / STD topo

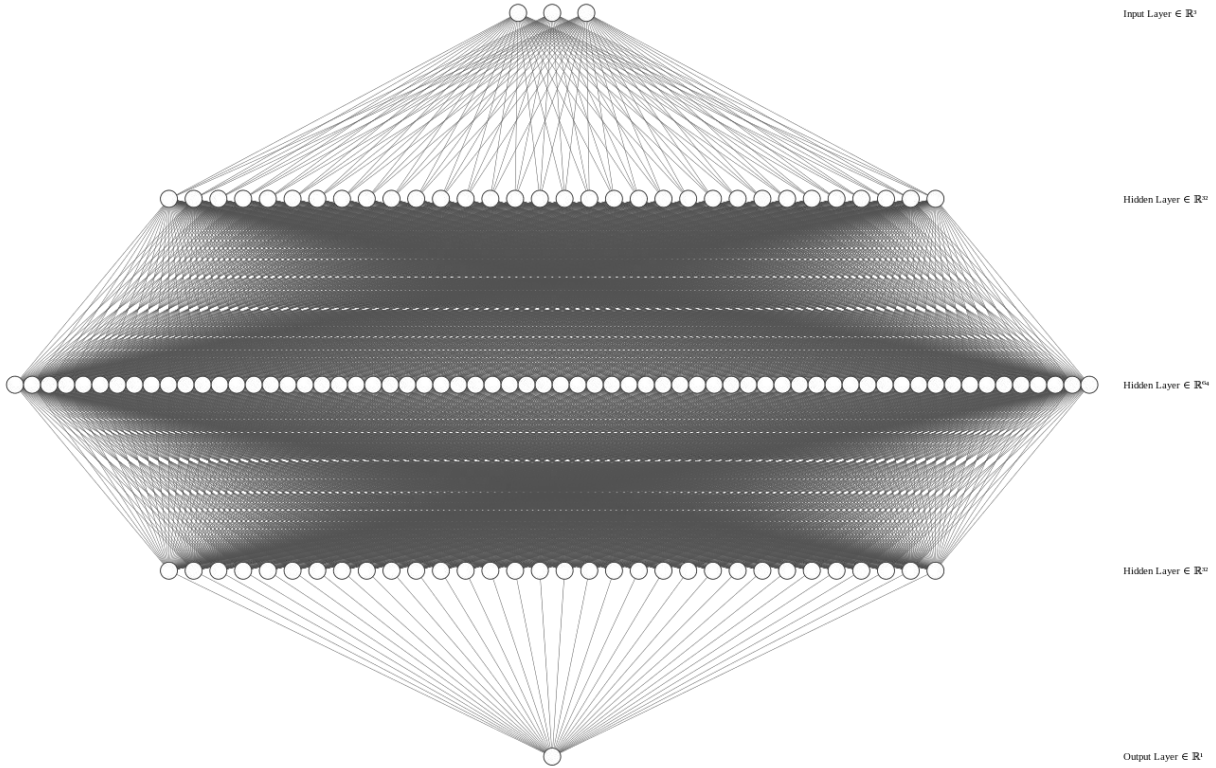

SCF

http://alexlenail.me/NN-SVG/index.html

Swenson and Lawrence (2012): commits 1, 2, 3, 4, thredds

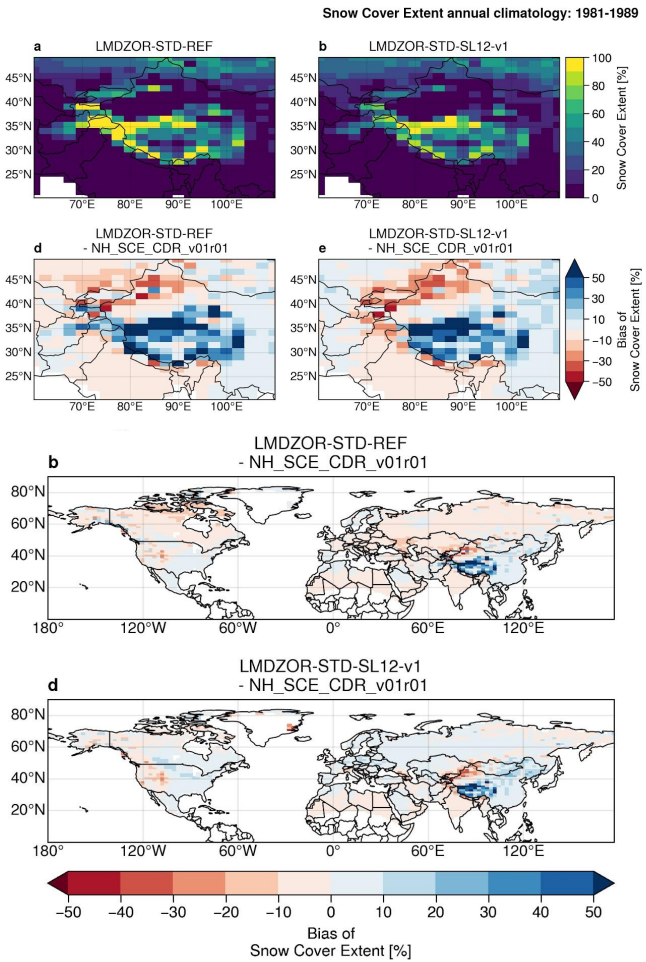

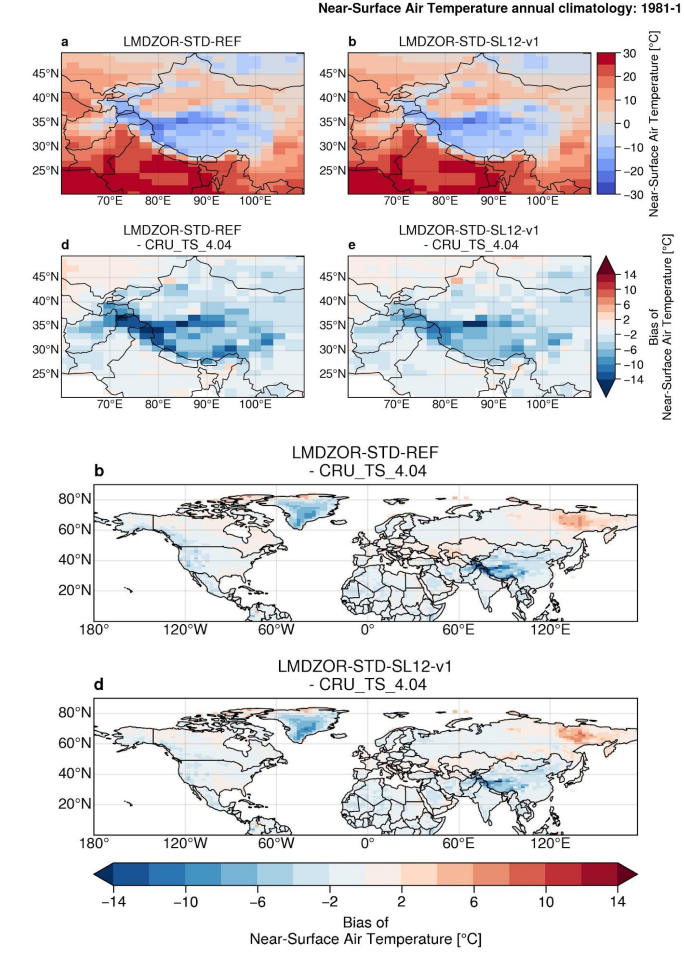

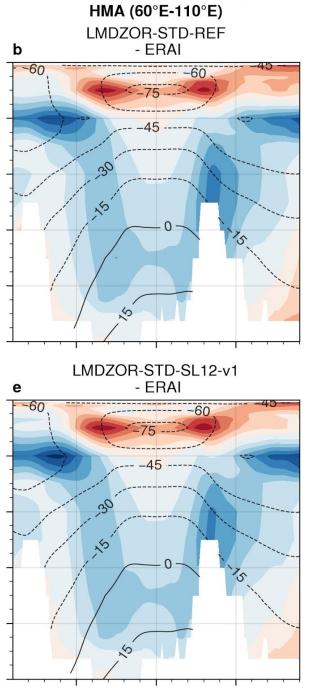

Roesch et al. (2001) without veget: code, thredds

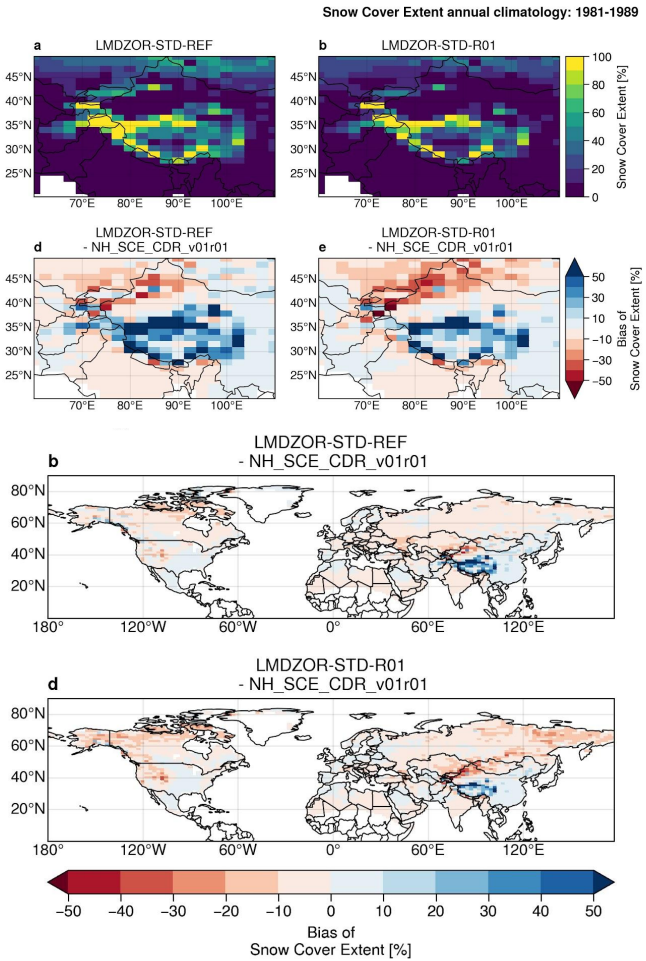

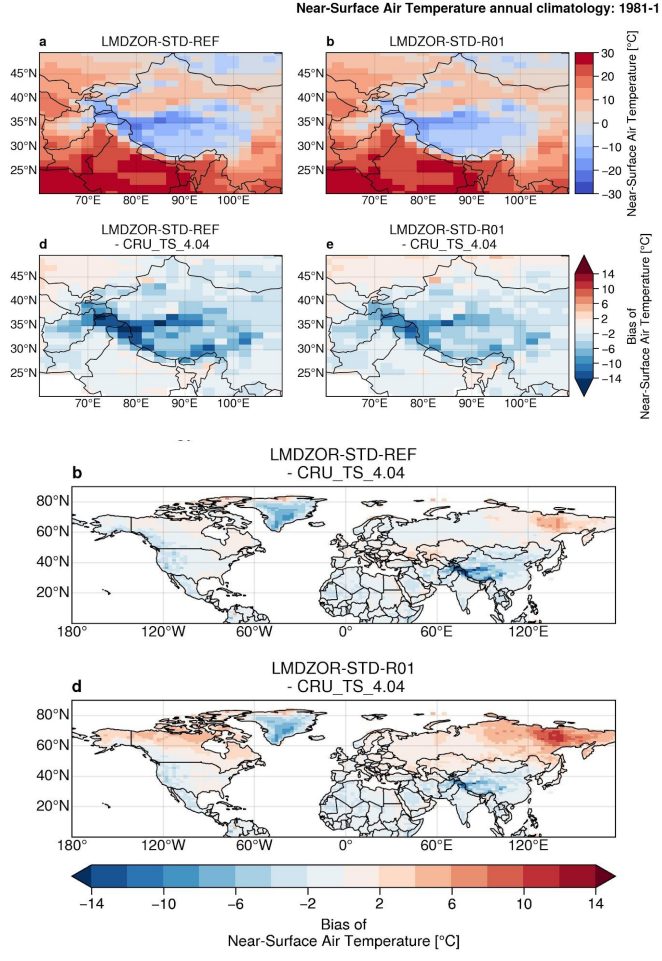

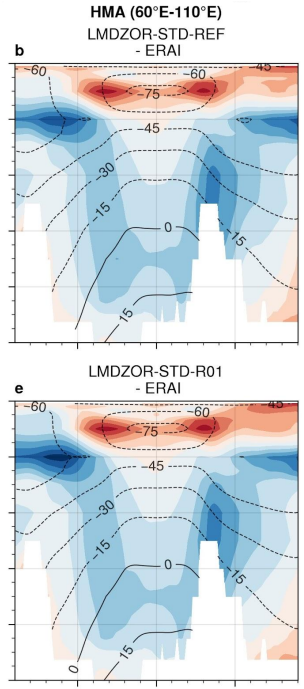

Permanent snow area: problem?

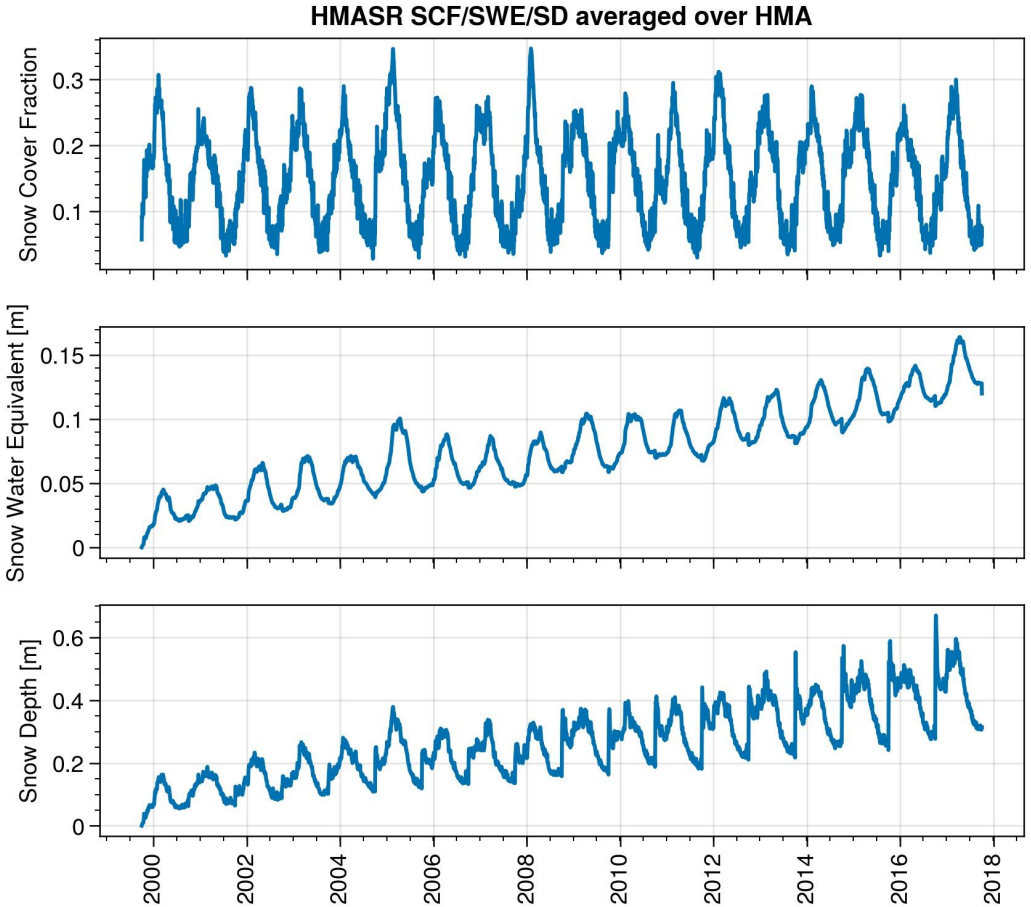

Dépôt aérosols

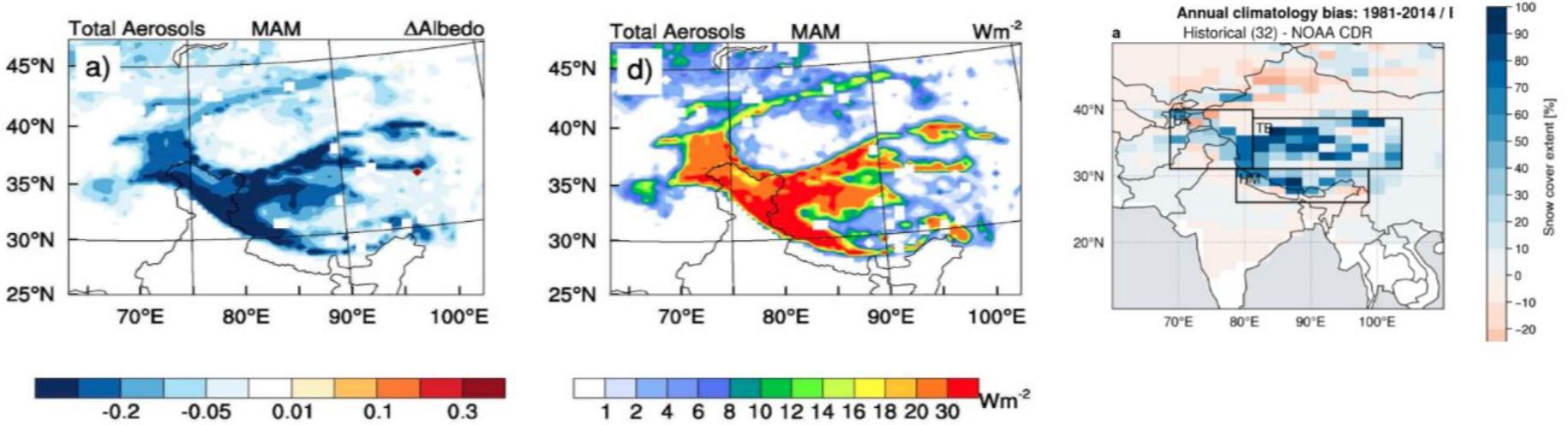

Usha et al., (2020, Fig 7)

TOFD

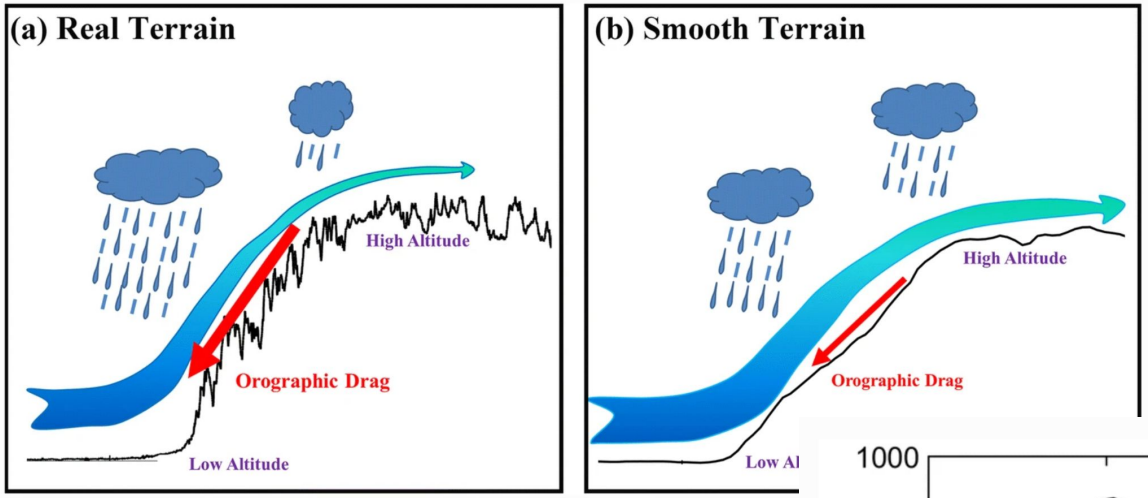

Wang et al., (2020, Fig 5 & 9)